
IS ONE LAYER ENOUGH? TRAINING A SINGLE TRANSFORMER LAYER CAN MATCH FULL-PARAMETER RL TRAINING

PREPRINT

Zijian ZhangUniversity of Minnesota
zha00175@umn.edu**Rizhen Hu**Peking University
xshrz123@gmail.com**Athanasios Glentis**University of Minnesota
glent007@umn.edu**Dawei Li**University of Minnesota
li004678@umn.edu**Chung-Yiu Yau**University of Minnesota
cyau@umn.edu**Hongzhou Lin ***Amazon
hongzhou.lin89@gmail.com**Mingyi Hong**University of Minnesota
mhong@umn.edu**ABSTRACT**

Reinforcement learning (RL) has become a central component of post-training large language models (LLMs), yet little is understood about how RL adaptation is distributed across transformer layers. Existing approaches typically update all model parameters uniformly, implicitly assuming that every layer contributes similarly to the gains obtained during RL post-training. In this work, we challenge this assumption through a systematic layer-wise study of RL training.

Surprisingly, we find that training **a single transformer layer** can recover most of the gains achieved by full-parameter RL training, and in some cases even surpass it. To quantify this phenomenon, we introduce the quantity *layer contribution*, which measures the fraction of full RL improvement recovered by training a layer in isolation. Across seven models spanning two model families (Qwen3, Qwen2.5), three RL algorithms (GRPO, GiGPO, Dr. GRPO), and multiple task domains including mathematical reasoning, code generation, and agentic decision-making, we observe a remarkably stable pattern: **RL gains are highly concentrated in a small subset of, and in many cases even a single, transformer layers**. More strikingly, the same structural pattern consistently emerges: high-contribution layers concentrate in the middle of the transformer stack, while layers near the input and output ends contribute substantially less. The resulting layer rankings remain strongly correlated across datasets, tasks, model families, and RL algorithms.

Our findings have two important implications. First, they reveal a previously unrecognized structural property of RL post-training: most RL gains are concentrated in a small subset of transformer layers rather than being uniformly distributed throughout the network. Second, they suggest new opportunities for improving RL training. Guided by the above observation, we develop simple layer-aware training strategies that consistently outperform standard full-parameter RL training, while ensembles of layer-specialized models provide additional gains through complementary behaviors. Together, our results provide new insights into how RL modifies large language models and suggest a new perspective for understanding and improving RL post-training.

1 Introduction

Reinforcement learning with verifiable rewards (RLVR) [Guo et al., 2025, Yang et al., 2025] has become a central component of post-training large language models (LLMs), driving substantial improvements in mathematical reasoning, code generation, and agentic decision-making [Yu et al., 2025, Shao et al., 2024]. While significant effort has been

*This work is independent of and outside of the work at Amazon

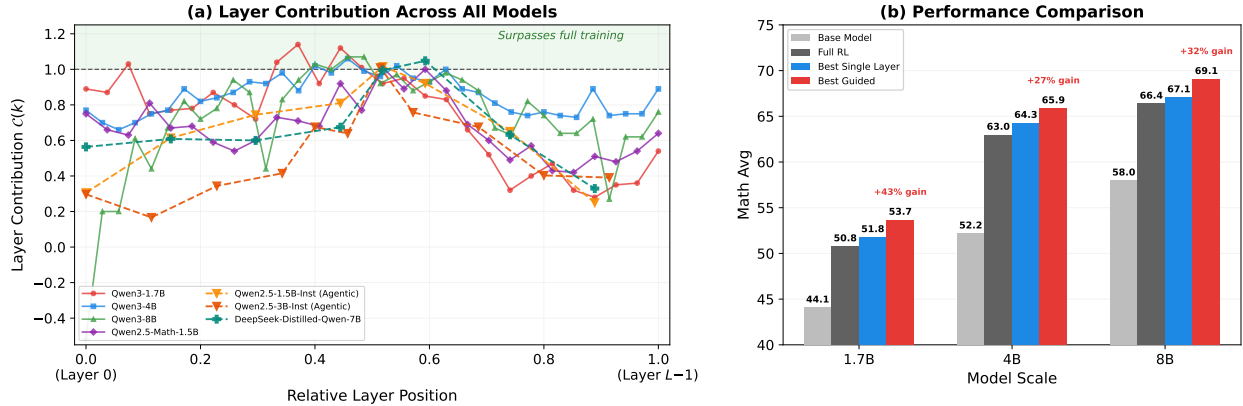


Figure 1: (a) Layer contribution (defined in §2.2) across all seven models studied in this work, plotted against depth-normalized relative layer position (0 = Layer 0, 1 = Layer $L-1$). Each point corresponds to RL training performed on a single transformer layer while all remaining layers are frozen. The y-axis measures the fraction of full-parameter RL improvement recovered by training that layer alone. Solid lines denote models with full layer scans; dashed lines denote models where a representative subset of layers is trained. Despite spanning two model families, three RL algorithms, and two task domains (mathematical reasoning and agentic tasks), all seven models exhibit the same structure: layers around 40%–60% of network depth consistently achieve the highest contribution, with some surpassing full-parameter RL training (green-shaded region). (b) Performance comparison on the three Qwen3 models (NuminaMath-CoT, math benchmarks). For each scale we show four bars: the base model, full-parameter RL, the best single-layer model, and *Best Guided*—the best result among the layer contribution-guided strategies from §4 (either boosting the learning rate of high-contribution layers or selectively training only those layers). The percentage annotations indicate the additional gain of Best Guided beyond full-parameter RL, expressed relative to the total RL gain. Training only these high-contribution layers consistently outperforms full-parameter RL across all three scales. Note that in (b), the full-parameter RL and Best Guided bars are averaged over 3 evaluation runs (§4); the full-parameter values therefore differ slightly from the single-run results reported in Table 2.

devoted to developing more effective RL objectives, reward models, and optimization algorithms, much less is known about a more fundamental question: **where, within the network, do the gains from RL actually emerge?** Existing RL post-training methods update all transformer layers jointly, providing little visibility into how different parts of a pretrained model contribute to the improvements achieved through RL. Understanding this layer-wise structure is important not only for explaining how RL reshapes a pretrained language model, but also for revealing whether RL adaptation possesses an underlying structure that can be exploited to further improve RL post-training.

In this work, we conduct a systematic layer-wise investigation of RL post-training. Surprisingly, we find that a single transformer layer can often recover most of the gains achieved by full-parameter RL training, and can sometimes even outperform it. This finding challenges the intuition that RL improvements arise from coordinated adaptation across the entire network. Instead, our results suggest that much of the benefit of RL post-training is concentrated in a surprisingly small subset of transformer layers.

Our study naturally connects to a growing body of work showing that pretrained LLMs are highly non-uniform across depth. Prior studies have demonstrated that transformer layers play markedly different roles: removing some layers causes severe degradation while others have relatively little effect [Zhang et al., 2024, Song et al., 2026, Nepal et al., 2025]. Similar layer-wise heterogeneity has also been observed during supervised finetuning, where both parameter updates and adaptation behaviors vary substantially across layers [Pan et al., 2024, Shi et al., 2025]. These observations have motivated a variety of layer-aware optimization strategies, including layer-wise sampling [Pan et al., 2024], adaptive layer selection [Liu et al., 2026, Kumar et al., 2025], and layer-aware alignment methods [Shi et al., 2025]. Notably, the layers identified as important often remain remarkably consistent across datasets and training settings [Shi et al., 2025], suggesting that pretrained LLMs possess stable layer-wise structural organization. However, these studies have focused primarily on inference-time behavior and supervised finetuning. Whether RL post-training exhibits a similarly structured pattern has remained largely unexplored.

To characterize this phenomenon, we conduct a systematic layer-wise study of RL post-training. For an LLM with L transformer layers, we independently train each layer using RL while freezing all remaining layers, and compare the resulting improvement with that achieved by standard full-parameter RL training. We introduce a simple metric

called *layer contribution*, which measures the fraction of full RL improvement that can be recovered by training a layer in isolation. This framework allows us to directly quantify the contribution of each layer to the gains achieved by RL post-training.

Our experiments reveal two striking findings. First, layer contributions vary dramatically across the network. The best individual layers recover up to 114% of the gains achieved by full-parameter RL training, while the weakest layers recover less than 30%. Second, this variation is highly structured rather than random. Across seven models spanning two model families (Qwen3, Qwen2.5), three RL algorithms (GRPO, GiGPO, Dr. GRPO), and three task domains including mathematical reasoning, code generation, and agentic decision-making, high-contribution layers consistently concentrate in the middle of the transformer stack, while layers near the input and output ends contribute substantially less. Further, for a fixed model, the per-layer contribution rankings themselves remain strongly correlated across training datasets (NuminaMath-CoT vs. DeepScaleR, Spearman $\rho = 0.76$) and even across tasks (NuminaMath-CoT vs. DeepCoder, Spearman $\rho = 0.59$; Figure 3). Together, these findings point to a previously unrecognized structural property of RL post-training: most RL gains are concentrated in a small subset of transformer layers.

These findings have two important implications. First, they reveal a previously unrecognized structural property of RL post-training. Contrary to the intuition that RL improvements arise from coordinated adaptation across the entire network, our results suggest that much of the benefit of RL post-training is concentrated in a small and stable subset of transformer layers. Second, this structure can be exploited algorithmically. Guided by layer contribution, we develop simple layer-aware training strategies that prioritize high-contribution layers and consistently outperform standard full-parameter RL training. For example, on Qwen3-8B, training only the ten highest-contribution layers achieves 69.1% average accuracy on mathematical reasoning benchmarks, compared to 66.4% achieved by full-parameter RL training. Furthermore, models trained on different layers exhibit complementary problem-solving behaviors, and combining them through majority voting yields additional gains beyond the full-parameter baseline.

In summary, our main contributions are:

- **RL adaptation is concentrated.** We show that RL gains are highly unevenly distributed across transformer layers. Remarkably, training a single layer can recover most of the gains achieved by full-parameter RL training and can sometimes even surpass it.
- **Layer contribution follows a consistent structure.** We introduce the notion of layer contribution and establish that high-contribution layers consistently concentrate in the middle of transformer networks across model scales, model families, RL algorithms, datasets, and task domains.
- **Implications for RL post-training.** We show that the discovered layer structure can be exploited to improve RL post-training. Simple layer-aware strategies that prioritize high-contribution layers consistently outperform standard full-parameter training, while even a profiling-free heuristic that trains only middle layers achieves comparable or better performance. Furthermore, models trained on different layers exhibit complementary behaviors, and combining them through majority voting yields additional gains beyond the full-parameter baseline.

2 Preliminaries

2.1 RLVR and GRPO

Reinforcement Learning with Verifiable Rewards (RLVR) optimizes a language model policy π_θ by maximizing expected reward on tasks with objectively verifiable answers. Given a prompt x , the model generates a response $y \sim \pi_\theta(\cdot|x)$, which is evaluated by a reward function $r(x, y)$ that returns a binary signal based on answer correctness.

In this work, we adopt Group Relative Policy Optimization (GRPO) [Shao et al., 2024], which estimates advantages without a learned value network. For each prompt x , GRPO samples a group of G responses $\{y_1, \dots, y_G\}$ from the current policy and computes a group-normalized advantage for each response:

$$\hat{A}_i = \frac{r(x, y_i) - \text{mean}(\{r(x, y_j)\}_{j=1}^G)}{\text{std}(\{r(x, y_j)\}_{j=1}^G)} \quad (1)$$

The policy is then updated by maximizing a clipped surrogate objective:

$$\mathcal{L}_{\text{GRPO}}(\theta) = \mathbb{E}_{x, \{y_i\}} \left[\frac{1}{G} \sum_{i=1}^G \left(\min \left(\rho_i \hat{A}_i, \text{clip}(\rho_i, 1 - \epsilon, 1 + \epsilon) \hat{A}_i \right) - \beta \mathbb{D}_{\text{KL}}[\pi_\theta \| \pi_{\text{ref}}] \right) \right] \quad (2)$$

where $\rho_i = \pi_\theta(y_i|x)/\pi_{\theta_{\text{old}}}(y_i|x)$ is the importance sampling ratio, β is the KL penalty coefficient, and π_{ref} is the fixed reference policy (the initial model before RL).

2.2 Single-Layer Training and Layer Contribution

To study how RL post-training interacts with different parts of a pretrained LLM, we adopt a controlled layer-wise training framework that isolates the adaptation behavior of each layer independently. For an LLM with L Transformer layers $\{\theta_0, \theta_1, \dots, \theta_{L-1}\}$, embedding parameters θ_{emb} , and language model head θ_{head} , standard full-parameter GRPO updates all parameters jointly by computing the gradient $\nabla_{\theta} \mathcal{L}_{\text{GRPO}}(\theta)$ over the full parameter set $\theta = \{\theta_{\text{emb}}, \theta_0, \dots, \theta_{L-1}, \theta_{\text{head}}\}$. In our single-layer training framework, we instead isolate a single layer θ_k and update only its parameters:

$$\theta_k \leftarrow \theta_k - \alpha \nabla_{\theta_k} \mathcal{L}_{\text{GRPO}}(\theta), \quad \text{all other parameters frozen.} \quad (3)$$

Note that the gradient $\nabla_{\theta_k} \mathcal{L}_{\text{GRPO}}(\theta)$ is computed via backpropagation through the full network, so it depends on all layers; only the parameter *update* is restricted to layer k . In practice, this is implemented in PyTorch by setting `requires_grad=False` for all parameters except those in the target layer θ_k . This procedure is repeated independently for every layer $k \in \{0, \dots, L-1\}$, isolating each layer’s ability to absorb RL-induced improvement. Each resulting model is then evaluated on the same set of in-domain benchmarks to obtain a performance score.

To quantify each layer’s capacity to capture RL-induced improvement, we define *layer contribution*. Let S_k denote the in-domain performance of the model trained on layer k , measured as the average score across in-domain benchmarks. Let S_{base} denote the performance of the original pretrained model without any RL training, and S_{full} denote the performance of the model after standard full-parameter GRPO training. The layer contribution of layer k is:

$$\mathcal{C}(k) = \frac{S_k - S_{\text{base}}}{S_{\text{full}} - S_{\text{base}}}. \quad (4)$$

A layer contribution of 1.0 indicates that single-layer training fully matches the gain of full-parameter training; values above 1.0 indicate that it surpasses full-parameter training; values near 0 indicate that the layer fails to capture meaningful RL improvements.

3 Measuring Layer Contribution in RLVR

We conduct systematic single-layer training experiments to examine whether different layers contribute equally to learning during RLVR. We study seven models spanning 1.5B to 8B parameters across two model families, three RL algorithms, and two task domains. We first describe the experimental setup and our protocol for ensuring fair comparison (§3.1), then present detailed layer contribution results on the Qwen3 models (§3.2), and finally establish the consistency of these findings across datasets (§3.3), model families, RL algorithms, and tasks (§3.4).

3.1 Experimental Setup and Fair Comparison

Models and training configurations. Our primary experiments use Qwen3-1.7B-Base (28 layers), Qwen3-4B-Base (36 layers), and Qwen3-8B-Base (36 layers) [Yang et al., 2025], which have not undergone post-training and thus provide a clean starting point for isolating the effects of RL. For each of these three models, we perform GRPO training on every layer independently using NuminaMath-CoT [LI et al., 2024] as the training dataset, with all other layers, embedding parameters, and the language model head frozen. A full-parameter GRPO baseline trained under identical hyperparameters serves as the reference. We choose this setting for our primary experiments because its difficulty level is well-suited to Qwen3 base models.

Further, to validate the generality of our findings beyond the Qwen3 family, NuminaMath-CoT dataset and GRPO algorithm, we additionally conduct experiments on Qwen2.5-Math-1.5B (28 layers) trained with Dr. GRPO [Liu et al., 2025], and Qwen2.5-1.5B-Instruct (28 layers) and Qwen2.5-3B-Instruct (36 layers) trained with GiGPO [Feng et al., 2025] on the agentic task ALFWorld [Shridhar et al., 2021], and DeepSeek-Distilled-Qwen-7B (28 layers) trained with GRPO on the Skywork [He et al., 2025] mathematics dataset.

In addition, to understand cross-dataset and cross-task consistency of layer contribution within a single and fixed model, beyond using the NuminaMath-CoT, we additionally train Qwen3-1.7B-Base with DeepScaleR [Luo et al., 2025b] (mathematics) and DeepCoder [Luo et al., 2025a] (coding).

Table 1 summarizes the seven models studied in this work. Note that in Table 1, the last column "Layer Scan" indicates if all the layers have been trained individually or only a selected subset of the layers are trained in our experiments.

Evaluation. For the primary Qwen3 experiments, we evaluate on 12 benchmarks spanning four categories: Math (MATH500, GSM8K, OlympiadBench, AMC) as the *in-domain evaluation*, and three out-of-domain categories, Code

Table 1: Summary of all models and training configurations studied in this work.

Model	Family	Params	Layers	RL Algorithm	Task / Dataset	Layer Scan
Qwen3-1.7B-Base	Qwen3	1.7B	28	GRPO	Math / NuminaMath-CoT	Full
Qwen3-4B-Base	Qwen3	4B	36	GRPO	Math / NuminaMath-CoT	Full
Qwen3-8B-Base	Qwen3	8B	36	GRPO	Math / NuminaMath-CoT	Full
Qwen2.5-Math-1.5B	Qwen2.5	1.5B	28	Dr. GRPO	Math / MATH	Full
Qwen2.5-1.5B-Instruct	Qwen2.5	1.5B	28	GiGPO	Agentic / ALFWorld	Partial
Qwen2.5-3B-Instruct	Qwen2.5	3B	36	GiGPO	Agentic / ALFWorld	Partial
DeepSeek-Distilled-Qwen-7B	Qwen2.5	7B	28	GRPO	Math / Skywork	Partial

(HumanEval+, MBPP, LiveCodeBench), Reasoning (GPQA-Diamond, MMLU-Pro), and Language (C-Eval, IFEval, MGSM). The overall score is computed as the unweighted average of the four category scores.

For the Qwen2.5-Math-1.5B experiment and DeepSeek-Distilled-Qwen-7B, we follow the evaluation protocol of Liu et al. [2025] and report results on six math benchmarks (AIME 2024, AIME 2025, AMC, MATH500, Minerva Math, OlympiadBench). For the agentic experiments, we evaluate on ALFWorld tasks. In the main text we report detailed in-domain results and out-of-distribution category averages; full per-benchmark breakdowns are provided in Appendix C.

Fair comparison of training methods. A key effort in our study is to ensure that when comparing single-layer training and full-parameter training, any observed differences reflect genuine layer-level variation rather than artifacts of suboptimal hyperparameters or premature convergence. Our detailed protocol is given below.

First, for each model, we tune the learning rate for the full-parameter baseline and select the value that yields the best performance; this ensures that the full-parameter reference is as strong as possible. Second, we apply this full-parameter-tuned learning rate to all single-layer training runs, so that no layer receives an unfair advantage or disadvantage from the learning rate choice. Third, all configurations, including full-parameter and single-layer, use identical hyperparameters for every other setting (batch size, KL coefficient, clip range, number of epochs) and are trained to convergence under the same training steps. This protocol ensures that when a single layer matches or surpasses full-parameter training, the comparison is rigorous: the full-parameter baseline is already at its best learning rate, and the single-layer run uses the same settings. Fourth, for a number of settings that have publicly available results using the same model, dataset, and methods, such as Dr. GRPO and GiGPO, we also report the best publicly available results, so as to best anchor our own full-parameter experiments and the performance achieved by layer-training.

Of course, since we only tuned the learning rate for full training but not the layer-wise training, a natural concern is whether low-contribution layers might improve with a larger learning rate, and if the high-contribution layer can be even better. We address this with a learning rate ablation study in Appendix A.7, which shows that adjusting the learning rate does not change the layer contribution rankings. Full training details and hyperparameter tables are provided in Appendix A.

3.2 Qwen3 Experiments: Layer Contribution Varies Dramatically

We begin by presenting detailed layer contribution results on the three Qwen3 models, NuminaMath-CoT dataset and using GRPO. We will conduct independent training on all 28 or 36 layers of these models. Figure 2 presents the per-layer contribution across model scales. Details of the hyperparameter tuning, including the tuning of the full-parameter baseline, are provided in Appendix A.

On Qwen3-1.7B-Base, layer contribution ranges from 0.28 (Layer 24) to 1.14 (Layer 10), with 5 out of 28 layers exceeding 1.0 and 7 layers falling below 0.5. The fact that a single layer can capture the entirety of the full training gain suggests that the effective change induced by RLVR can be captured within the parameter subspace of a single layer. Moreover, that some layers individually surpass full-parameter training suggests that when all layers are trained jointly, certain layers learn less effectively and may dilute the overall improvement. At the other end, layers with contribution below 0.5 have limited capacity to learn from RL signals in isolation. The variation across layers is not marginal but dramatic, with the best layer capturing over four times the gain of the worst.

Similar patterns emerge on larger models. On Qwen3-4B-Base, contribution ranges from 0.66 (Layer 2) to 1.06 (Layer 16), with 4 layers reaching or exceeding 1.0. On Qwen3-8B-Base, the best layers again reach contributions above 1.0 (Layer 16, $C = 1.07$), while most layers fall in the range of 0.6 to 1.0. A notable exception is Layer 0 on Qwen3-8B-Base, which exhibits a negative contribution ($C = -0.51$), indicating that training this layer in isolation

Table 2: Per-layer training results on the three Qwen3 models. We report each in-domain math benchmark, three out-of-distribution category averages (Code, Reasoning, Language), and the overall average across all four categories. C_{math} and C_{all} denote layer contribution computed on the in-domain math average and the overall average, respectively. Complete per-layer results are in Appendix C.

Model	Setting	In-domain (Math)						Out-of-distribution			Overall	C_{all}
		MATH500	GSM8K	Olymp.	AMC	Avg	C_{math}	Code	Reas.	Lang.		
Qwen3-1.7B-Base	Base	57.4	74.4	18.7	26.1	44.1	0.00	34.9	20.7	41.7	35.4	0.00
	Full	64.0	82.0	26.9	30.2	50.8	1.00	33.5	22.6	48.2	38.8	1.00
	Layer 10	68.6	80.5	27.3	30.8	51.8	1.14	34.6	21.9	47.2	38.9	1.03
	Layer 12	65.6	81.3	27.3	32.4	51.6	1.12	36.2	21.5	47.4	39.2	1.12
	Layer 1	64.4	79.4	25.9	30.2	50.0	0.87	40.0	22.7	47.1	39.9	1.32
	Layer 7	64.0	80.1	24.9	29.0	49.5	0.80	38.1	22.4	46.5	39.1	1.09
	Layer 24	60.6	74.8	21.2	27.6	46.1	0.28	30.6	21.6	44.2	35.6	0.06
Qwen3-4B-Base	Base	65.2	75.4	27.6	40.5	52.2	0.00	41.5	28.8	57.6	45.0	0.00
	Full	77.2	91.9	38.4	47.1	63.7	1.00	48.8	32.4	62.9	51.9	1.00
	Layer 16	79.4	92.0	40.3	45.5	64.3	1.06	51.9	33.0	64.4	53.4	1.22
	Layer 14	78.4	90.3	39.9	46.5	63.8	1.02	52.9	31.6	63.3	52.9	1.14
	Layer 11	76.6	90.5	36.2	47.6	62.7	0.92	51.3	33.8	62.8	52.7	1.12
	Layer 24	77.0	89.5	38.5	43.6	62.2	0.87	47.4	31.9	61.7	50.8	0.84
	Layer 2	73.8	87.7	35.3	42.4	59.8	0.66	49.1	31.9	62.3	50.8	0.84
Qwen3-8B-Base	Base	71.8	82.0	36.6	41.7	58.0	0.00	50.4	32.2	57.5	49.5	0.00
	Full	80.0	92.3	42.8	50.8	66.5	1.00	53.7	35.5	63.7	54.9	1.00
	Layer 16	80.4	91.8	44.1	52.0	67.1	1.07	54.5	35.5	68.8	56.5	1.30
	Layer 15	79.8	92.8	40.6	52.7	66.5	1.00	56.8	34.0	68.9	56.5	1.30
	Layer 8	77.0	89.0	41.5	50.9	64.6	0.78	54.3	34.4	62.0	53.8	0.80
	Layer 2	72.8	84.6	38.5	43.0	59.7	0.20	51.4	33.7	59.4	51.1	0.30
	Layer 0	61.8	79.6	31.0	42.4	53.7	-0.51	44.0	34.0	63.0	48.7	-0.15

actually degrades math performance below the base model. Across all three model scales, middle layers consistently exhibit higher contribution, while layers near the input and output ends contribute less (Table 2).

Interestingly, high-contribution layers do not merely improve on the in-domain training objective, as they also improve out-of-distribution capabilities. To show this, we compute an *overall* layer contribution $C_{\text{all}}(k)$ using the same formula as Equation (4) but replacing the in-domain math score with the overall score (the unweighted average of all four category scores: Math, Code, Reasoning, and Language; see Table 2). As shown in Figure 2, C_{all} closely tracks C_{math} across layers (Pearson $r > 0.6$ on all three scales): layers that learn math effectively also tend to improve on out-of-distribution tasks including coding, reasoning, and language understanding. This indicates that single-layer training captures genuine, broad capability improvement rather than overfitting to the training objective, and that layer contribution reflects a general property of each layer rather than a task-specific one.

3.3 Qwen3 Experiments: Layer Contribution is Consistent Across Datasets and Tasks

A natural question is whether the layer contribution patterns observed in §3.2 are specific to the training dataset, or reflect a more fundamental property of the model. To test this, we repeat our single-layer training experiments on Qwen3-1.7B-Base using two additional datasets: DeepScaleR [Luo et al., 2025b], a mathematics dataset, and DeepCoder [Luo et al., 2025a], a coding dataset.

We first compare layer contribution across two math datasets: NuminaMath-CoT and DeepScaleR. For each dataset, we compute the layer contribution $C(k)$ for all 28 layers and rank them accordingly. We then measure the consistency between the two rankings using the Spearman rank correlation coefficient, which captures whether the relative ordering of layers is preserved regardless of differences in absolute contribution values. Despite differences in data composition and difficulty, the per-layer contribution rankings are strongly correlated (Spearman $\rho = 0.76$, $p < 0.001$). Figure 3(a) visualizes this correspondence: each point represents a single layer, and layers that rank highly under one dataset consistently rank highly under the other. This suggests that layer contribution is not driven by the specific content of the training data, but by the model’s internal structure.

We further test whether this consistency extends across tasks by comparing NuminaMath-CoT (math) and DeepCoder (code), which target fundamentally different capabilities. The per-layer rankings remain correlated (Spearman $\rho = 0.59$,

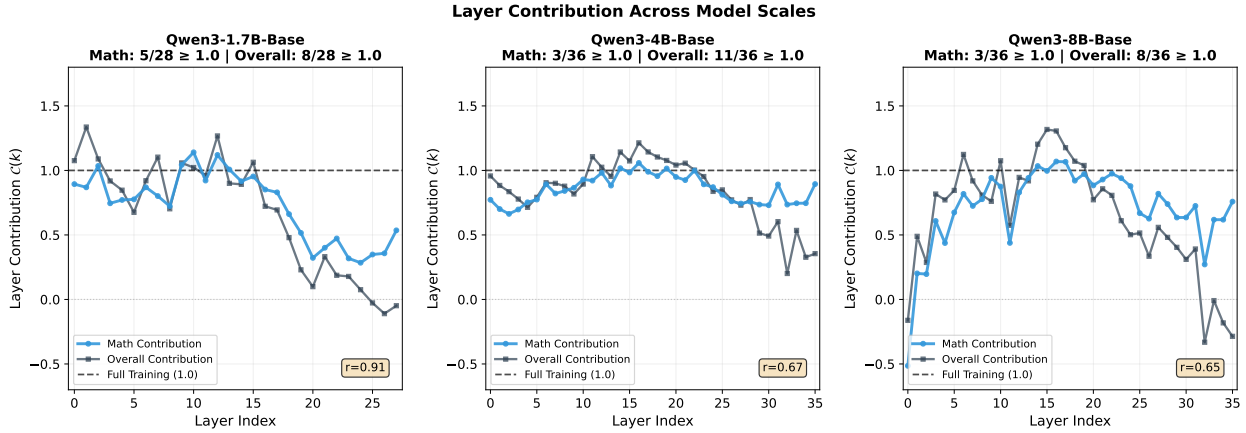


Figure 2: Layer contribution $\mathcal{C}(k)$ across model scales. Blue: math contribution (in-domain). Black: overall contribution (averaged across all capabilities). Dashed line indicates full-parameter training ($\mathcal{C} = 1.0$). Each point represents one layer trained in isolation. Math and overall contribution closely track each other across layers (Pearson $r > 0.6$ on 1.7B,4B and 8B), indicating that high-contribution layers achieve broad capability improvement rather than overfitting to the training objective. Across all three scales, middle layers consistently exhibit higher contribution.

Cross-Dataset Consistency of Layer Contribution (Qwen3-1.7B-Base)

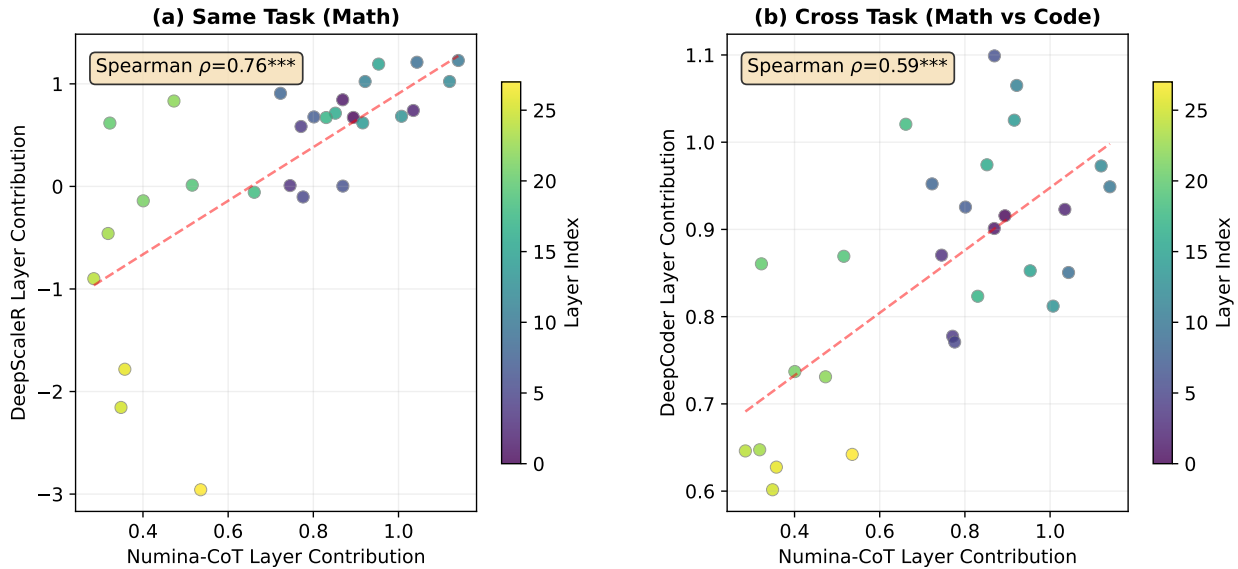


Figure 3: Cross-dataset consistency of layer contribution on Qwen3-1.7B-Base. Each point represents a single layer. (a) NuminaMath-CoT vs. DeepScaleR (both math). (b) NuminaMath-CoT (math) vs. DeepCoder (code).

$p < 0.001$; Figure 3(b)), indicating that even when the training objective changes from mathematical reasoning to code generation, the same layers tend to have the highest contribution.

Taken together, these results establish that layer contribution is an intrinsic property of the pretrained model, determined by its pretrained weights rather than the specific training data or task. This has a direct practical implication: layer selections derived from a smaller or more accessible dataset can be reliably transferred to guide training on other data, a possibility we explore in §4.

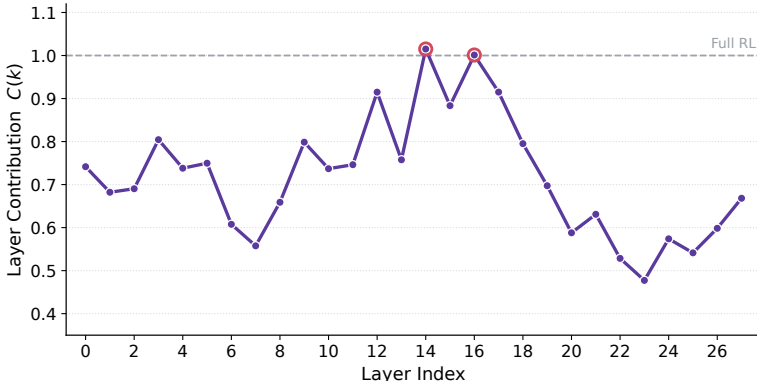


Figure 4: Layer contribution $C(k)$ for Qwen2.5-Math-1.5B (28 layers) trained with Dr. GRPO. Each point corresponds to one transformer layer trained in isolation. The dashed line marks full-parameter training ($C = 1.0$); circled markers indicate layers that reach or exceed it. Despite the change in both model family and RL algorithm, the contribution profile retains the same structure observed on Qwen3: middle layers contribute most, while layers near the input and output ends contribute less.

Table 3: Per-layer training results on Qwen2.5-Math-1.5B (Dr. GRPO). We report each math benchmark and the overall average over the six benchmarks (Avg). C denotes layer contribution computed on Avg. Complete per-layer results are in Appendix C. †Official result from Liu et al. [2025].

Setting	AIME	AIME25	AMC	MATH500	Minerva	Olymp.	Avg	C
Base	20.0	6.7	32.5	33.0	12.5	22.8	21.2	0.00
Full	16.7	10.0	51.8	74.4	25.0	38.8	36.1	1.00
Dr. GRPO†	20.0	6.7	53.0	74.2	25.7	37.6	36.2	–
Layer 14	20.0	10.0	52.3	74.8	25.6	35.3	36.3	1.01
Layer 16	20.0	10.0	51.8	75.2	24.9	34.9	36.1	1.00
Layer 12	20.0	10.0	45.8	73.8	25.0	34.8	34.9	0.92
Layer 8	13.3	3.3	43.4	69.4	20.6	30.7	30.1	0.60
Layer 23	10.0	3.3	38.6	64.0	19.9	29.3	27.5	0.42

3.4 Generalization Across Model Families, Algorithms, and Tasks

The consistency observed in §3.3 shows that layer contribution is robust to changes in the training data and task within a single model. A stronger test is whether the phenomenon persists when the model family, the RL algorithm, or the task domain changes. We examine each of these axes below.

Different model family and RL algorithm (Qwen2.5-Math-1.5B, Dr. GRPO). We first test whether the findings transfer when both the model family and the RL algorithm change simultaneously. We repeat our single-layer training experiments on Qwen2.5-Math-1.5B, a model from a different family and pretraining recipe than the Qwen3 models studied above, and replace GRPO with Dr. GRPO [Liu et al., 2025] as the optimization algorithm, following its training recipe (full details in Appendix A.3). This setup differs from our main experiments along two independent axes.

Figure 4 and Table 3 show the results. The qualitative structure is identical to that of the Qwen3 models in §3.2: layer contribution rises toward the middle of the network and falls off near both ends. The highest-contribution layers are concentrated in the middle of the stack (Layer 14, $C = 1.01$; Layer 16, $C = 1.00$; Layer 12, $C = 0.92$; Layer 15, $C = 0.89$; Layer 17, $C = 0.88$), whereas the lowest-contribution layers lie toward the later part of the network (Layer 23, $C = 0.42$; Layer 22, $C = 0.43$; Layer 25, $C = 0.48$). The best layer again recovers more than twice the contribution of the worst, reproducing the dramatic layer-wise variation seen on Qwen3. Moreover, a couple of middle layers (Layers 14 and 16) reach or slightly exceed the full-parameter baseline ($C \geq 1.0$), echoing our earlier finding that single-layer training can match or surpass full-parameter RL.

Different task domain: agentic tasks (Qwen2.5-Instruct, GiGPO, ALFWorld). The experiments above focus on mathematical reasoning and code generation. To test whether layer contribution generalizes to a fundamentally

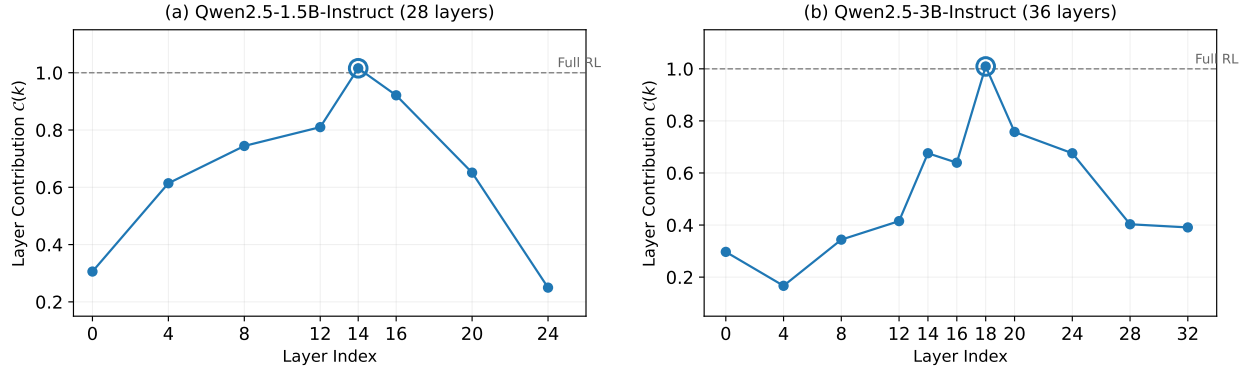


Figure 5: Layer contribution $\mathcal{C}(k)$ on the agentic task ALFWorld, trained with GiGPO. (a) Qwen2.5-1.5B-Instruct (28 layers). (b) Qwen2.5-3B-Instruct (36 layers). A representative subset of layers is trained due to computational constraints. The dashed line marks full-parameter training ($\mathcal{C} = 1.0$); circled markers indicate layers that reach or exceed it. Despite the shift from mathematical reasoning to multi-step agentic decision-making, and the change in model family and RL algorithm, the contribution profile retains the same middle-layer concentration structure: Layer 14 ($\mathcal{C} = 1.02$) on the 1.5B model and Layer 18 ($\mathcal{C} = 1.01$) on the 3B model each surpass full-parameter training, while early and late layers contribute substantially less.

Table 4: Per-layer training results on Qwen2.5-1.5B-Instruct (GiGPO, ALFWorld). We report success rate (%) on each ALFWorld task category and the overall average. \mathcal{C} denotes layer contribution computed on the overall score. A representative subset of layers is trained. [†]Official result from Feng et al. [2025].

Setting	Pick&Place	Pick2&Place	LookInLight	Heat&Place	Cool&Place	Clean&Place	Overall	\mathcal{C}
Base	5.9	0.0	5.5	9.7	4.2	3.3	4.1	0.00
Full	100	81.0	91.7	83.3	81.8	88.9	87.8	1.00
GiGPO [†]	94.4	76.4	67.5	94.4	79.8	94.8	86.7	–
Layer 14	100	85.7	100	83.3	81.8	77.8	89.1	1.02
Layer 16	91.9	52.4	91.7	94.4	72.7	83.3	81.2	0.92
Layer 12	83.8	47.6	66.7	72.2	81.8	66.7	71.9	0.81
Layer 8	75.7	47.6	66.7	66.7	63.6	72.2	66.4	0.74
Layer 20	67.6	47.6	66.7	50.0	50.0	66.7	58.6	0.65
Layer 4	59.5	42.9	75.0	55.6	50.0	55.6	55.5	0.61
Layer 0	48.6	23.8	41.7	16.7	13.6	22.2	29.7	0.31
Layer 24	32.4	19.0	41.7	11.1	18.2	27.8	25.0	0.25

different task domain, we conduct single-layer training on Qwen2.5-1.5B-Instruct (28 layers) and Qwen2.5-3B-Instruct (36 layers) using GiGPO on the agentic benchmark ALFWorld. Unlike the mathematical setting, agentic tasks require multi-step decision-making in interactive environments, representing a qualitatively different capability.

Despite the change in task domain, model family, and RL algorithm relative to our main Qwen3 experiments, the same structural pattern emerges (Figure 5). On Qwen2.5-1.5B-Instruct, the best single layer (Layer 14) achieves $\mathcal{C} = 1.02$, surpassing full-parameter training, while the weakest layer (Layer 24) reaches only $\mathcal{C} = 0.25$ (Table 4). High-contribution layers again concentrate in the middle of the network. On Qwen2.5-3B-Instruct, the pattern is consistent: the best layer (Layer 18) reaches $\mathcal{C} = 1.01$, again surpassing full-parameter training, while the weakest (Layer 4) reaches only $\mathcal{C} = 0.17$ (Table 5). Notably, the RL gain on these agentic tasks is far larger than in the mathematical setting (83.7 and 66.0 points respectively, compared to 6–10 points on math), yet the middle-layer concentration structure persists, indicating that the pattern is not limited to small-magnitude adaptations. These results demonstrate that the layer contribution structure is not specific to reasoning or coding tasks but extends to agentic problem-solving.

Different model architecture (DeepSeek-Distilled-Qwen-7B, GRPO, Skywork). To further test generality beyond the Qwen3 model families, we conduct partial-layer experiments on DeepSeek-Distilled-Qwen-7B (28 layers), a model distilled from DeepSeek-R1 into the Qwen architecture. We train with GRPO on the Skywork [He et al., 2025] mathematics dataset.

Table 5: Per-layer training results on Qwen2.5-3B-Instruct (GiGPO, ALFWorld). We report success rate (%) on each ALFWorld task category and the overall average. \mathcal{C} denotes layer contribution computed on the overall score. A representative subset of layers is trained.

Setting	Pick&Place	Pick2&Place	LookInLight	Heat&Place	Cool&Place	Clean&Place	Overall	\mathcal{C}
Base	57.6	9.1	37.5	0.0	12.5	8.0	24.2	0.00
Full	100	81.0	75.0	83.3	86.4	100	90.2	1.00
Layer 18	94.6	76.2	100	83.3	86.4	100	90.8	1.01
Layer 20	97.3	52.4	100	33.3	77.3	72.2	74.2	0.76
Layer 14	89.2	52.4	75.0	38.9	68.2	72.2	68.8	0.68
Layer 24	97.3	47.6	58.3	55.6	54.5	72.2	68.8	0.68
Layer 16	91.9	52.4	50.0	50.0	63.6	61.1	66.4	0.64
Layer 12	78.4	28.6	66.7	44.4	40.9	33.3	51.6	0.42
Layer 28	79.5	36.8	44.4	27.3	32.0	48.0	50.8	0.40
Layer 32	81.1	42.9	50.0	22.2	36.4	38.9	50.0	0.39
Layer 8	81.1	28.6	50.0	33.3	27.3	33.3	46.9	0.34
Layer 0	78.4	28.6	41.7	38.9	18.2	27.8	43.8	0.30
Layer 4	67.6	28.6	41.7	22.2	18.2	5.6	35.2	0.17

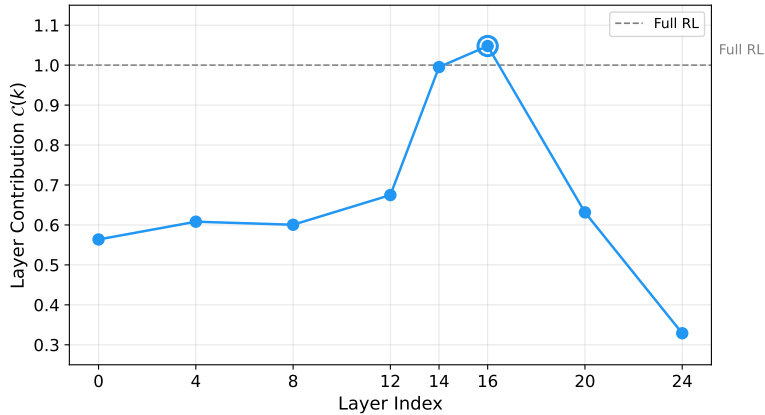


Figure 6: Layer contribution $\mathcal{C}(k)$ for DeepSeek-Distilled-Qwen-7B (28 layers) trained with GRPO on the Skywork mathematics dataset. Only a subset of layers (0, 4, 8, 12, 14, 16, 20, 24) are trained due to computational constraints. The dashed line marks full-parameter training ($\mathcal{C} = 1.0$); the circled marker indicates the layer that exceeds it. Despite differing from the Qwen3 and Qwen2.5 models in both pretraining recipe (distilled from DeepSeek-R1) and training data, the contribution profile retains the same middle-layer concentration structure: Layer 16 ($\mathcal{C} = 1.05$) surpasses full-parameter training, while early and late layers contribute substantially less.

The same structure reappears: middle layers exhibit the highest contribution, with the best layer reaching $\mathcal{C} = 1.05$ and the weakest reaching $\mathcal{C} = 0.33$. The best single layer again surpasses full-parameter training. This confirms that the phenomenon is not confined to models pretrained from scratch but also holds for distilled models.

Summary across all seven models. Table 7 summarizes the key layer contribution statistics across all seven models. Despite variation in model family, scale, RL algorithm, training dataset, and task domain, every model exhibits the same qualitative structure: (1) the best single layer matches or surpasses full-parameter training ($\mathcal{C} \geq 1.0$), (2) high-contribution layers concentrate in the middle of the network, and (3) layers near the input and output ends contribute substantially less.

These results, together with the cross-dataset and cross-task consistency established in §3.3, demonstrate that the observed layer contribution pattern is remarkably stable. Across seven models spanning two model families, three RL algorithms, multiple datasets, three task domains, and model scales from 1.5B to 8B, the same qualitative behavior consistently emerges: RL gains are highly uneven across transformer layers, concentrate in the middle of the network, and can often be largely recovered by training only a single layer. Collectively, these findings suggest that the gains

Table 6: Per-layer training results on DeepSeek-Distilled-Qwen-7B (GRPO, Skywork). We report each math benchmark and the overall average over six benchmarks (Avg). \mathcal{C} denotes layer contribution computed on Avg. Due to computational constraints, we train a representative subset of layers spanning the full depth of the network.

Setting	AIME	AIME25	AMC	MATH500	Minerva	Olymp.	Avg	\mathcal{C}
Base	47.2	35.3	69.9	88.2	34.6	49.0	54.1	0.00
Full	55.0	45.0	83.1	94.0	41.2	68.7	64.5	1.00
Layer 16	57.5	45.0	86.7	96.6	38.6	65.6	65.0	1.05
Layer 14	55.0	38.3	86.7	95.6	43.4	67.7	64.5	1.00
Layer 12	53.3	37.1	81.9	92.8	39.3	62.2	61.1	0.67
Layer 20	57.9	36.7	77.1	93.0	40.4	58.8	60.6	0.63
Layer 4	50.8	37.5	81.9	93.2	39.7	59.3	60.4	0.61
Layer 8	51.2	37.5	79.5	91.4	42.3	60.0	60.3	0.60
Layer 0	50.4	35.4	83.1	93.2	38.2	59.3	59.9	0.56
Layer 24	52.5	35.4	73.5	90.8	37.6	55.1	57.5	0.33

Table 7: Layer contribution summary across all seven models. For each model we report the best and worst layer contribution, the number of layers with $\mathcal{C} \geq 1.0$, and whether the contribution profile exhibits a middle-layer concentration shape. All models show the same qualitative pattern. [†]Only a representative subset of layers is trained.

Model	Family	Algorithm	Task	Best \mathcal{C}	Worst \mathcal{C}	Layers ≥ 1.0	Middle-layer concentration
Qwen3-1.7B-Base	Qwen3	GRPO	Math	1.14	0.28	5/28	✓
Qwen3-4B-Base	Qwen3	GRPO	Math	1.06	0.66	4/36	✓
Qwen3-8B-Base	Qwen3	GRPO	Math	1.07	-0.51	4/36	✓
Qwen2.5-Math-1.5B	Qwen2.5	Dr. GRPO	Math	1.01	0.42	2/28	✓
Qwen2.5-1.5B-Instruct	Qwen2.5	GiGPO	Agentic	1.02	0.25	1/8 [†]	✓
Qwen2.5-3B-Instruct	Qwen2.5	GiGPO	Agentic	1.01	0.17	1/11 [†]	✓
DeepSeek-Distilled-Qwen-7B	Qwen2.5	GRPO	Math	1.05	0.33	2/8 [†]	✓

from RL post-training emerge primarily through the adaptation of a relatively small subset of transformer layers, rather than through uniform adaptation across the entire network.

4 Guiding Full-Parameter RLVR by Layer Contribution

The experiments in §3 establish that layers differ dramatically in contribution. This raises a practical question: *Can this observation be used to improve standard full-parameter RLVR, which treats all layers uniformly during training?* Since different layers vary in their capacity to absorb RL training signals, differentiating across layers according to their contribution should yield better outcomes than uniform treatment. We explore three strategies: adjusting per-layer learning rates based on layer contribution (§4.1), selectively training only the highest-contribution layers (§4.2), and a heuristic method for selective training based on layer position (§4.3). All experiments in this section use NuminaMath-CoT as the training dataset and report math performance averaged over the same four in-domain benchmarks (MATH500, GSM8K, OlympiadBench, AMC) as in §3, unless otherwise noted. All results are reported as mean \pm standard deviation over 3 independent evaluation runs.

4.1 Layer-Adaptive Learning Rate

Standard full-parameter RLVR applies a uniform learning rate across all layers. However, since layers differ substantially in their capacity to learn from RL signals, a uniform learning rate may be suboptimal. We therefore experiment with assigning higher learning rates to high-contribution layers while keeping other layers at the base learning rate.

Specifically, we select the best k layers ranked by layer contribution (denoted Bk , e.g., $B5$ = the 5 highest-contribution layers) and increase their learning rate to 1×10^{-5} , while all remaining layers are trained at the default rate 5×10^{-6} . As a control experiment, we also boost the worst k layers (denoted Wk). We experiment with $k \in \{5, 10\}$ across all three model scales (Figure 7). Across models and configurations, boosting high-contribution layers consistently improves math performance over the uniform-lr baseline: on Qwen3-1.7B-Base, Boost B10 achieves 53.70 ± 0.40 compared to the 50.82 ± 0.40 baseline (+2.88, representing 43% of the total RL training gain); on Qwen3-4B-Base, our B10 gets 64.42 ± 0.13 vs. 62.97 ± 0.78 (+1.45); and on Qwen3-8B-Base, Boost B10 reaches 67.42 ± 0.40 vs.

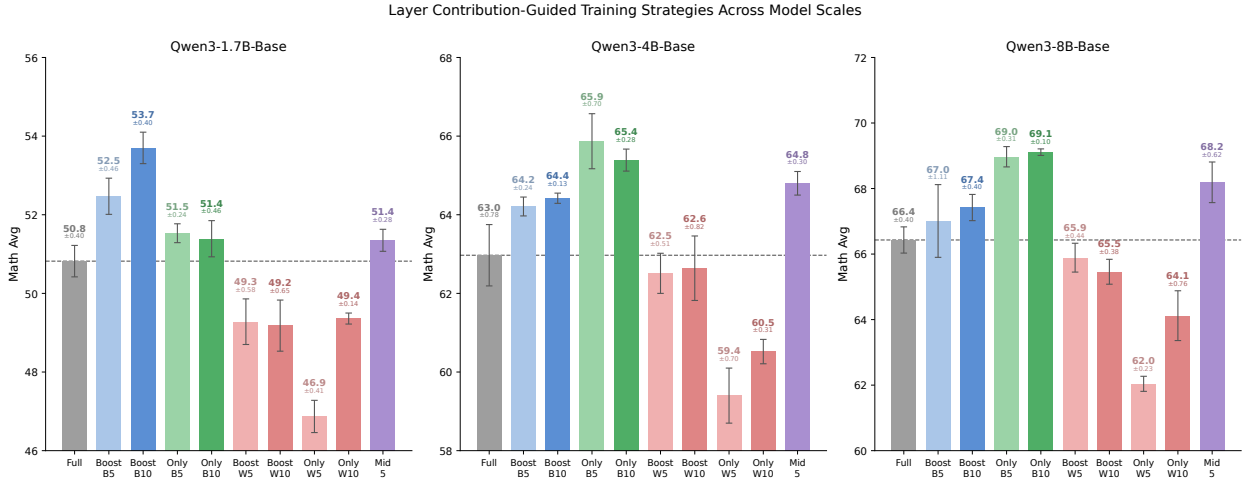


Figure 7: Layer contribution-guided training strategies across model scales. **Blue**: boosting high-contribution layers with increased learning rate. **Green**: training only high-contribution layers. **Red**: control experiments using low-contribution layers. **Purple**: position-based middle-layer heuristic. **Grey**: full-parameter baseline (also indicated by dashed line). **Bk/Wk**: Best/Worst k layers by layer contribution. Error bars denote one standard deviation over 3 independent training runs.

$66.43 \pm 0.40 (+0.99)$. In contrast, boosting the lowest-contribution layers (Boost Wk) leads to a decline in performance across all three models. This asymmetry confirms that the improvement is driven by the contribution-guided selection rather than the learning rate adjustment itself.

4.2 Layer-Selective Training

We further ask whether low-contribution layers can be frozen entirely during training. We train only the best k layers while keeping all remaining layers frozen, with $k \in \{5, 10\}$ across all three model scales (Figure 7).

On Qwen3-1.7B-Base, training only the best layers already exceeds the full-parameter baseline (Only B5: 51.53 ± 0.24 , Only B10: 51.39 ± 0.46 , vs. baseline 50.82 ± 0.40). On larger models, the improvement is more pronounced: on Qwen3-4B-Base, Only B5 reaches $65.87 \pm 0.70 (+2.90)$ over baseline, representing 27% of the total RL gain, and on Qwen3-8B-Base, Only B10 reaches $69.11 \pm 0.10 (+2.68)$, representing 32% of the total RL gain. In both cases, selective training surpasses not only full-parameter training but also the adaptive learning rate strategy from §4.1. This suggests that at larger scales, updates to low-contribution layers may not contribute positively to training, and freezing them yields a cleaner optimization. Conversely, training only the worst k layers leads to substantially worse results across all scales (e.g., Only W5: 46.87 ± 0.41 on 1.7B, 59.40 ± 0.70 on 4B, 62.04 ± 0.23 on 8B), confirming that the effective learning in RLVR is concentrated in high-contribution layers.

4.3 Heuristic Layer Selection

The preceding strategies require layer contribution rankings derived from per-layer training, which is expensive and impractical for routine use. We explore whether this profiling step can be bypassed altogether. Since layer contribution consistently exhibits a pattern of higher values in middle layers and lower values near the input and output ends across all three model scales (Figure 2), we test a simple heuristic: select the middle k layers by position, without any profiling at all.

Specifically, for a model with L layers, we select layers in the range $[\lfloor L/2 - k/2 \rfloor, \lfloor L/2 + k/2 \rfloor]$ and apply the same selective training setup as in §4.2. Setting $k = 5$ yields layers 11–15 for Qwen3-1.7B-Base ($L = 28$) and layers 15–19 for both Qwen3-4B-Base and Qwen3-8B-Base ($L = 36$). On Qwen3-1.7B-Base, heuristic selection of the middle 5 layers achieves a math performance of 51.35 ± 0.28 , compared to 51.53 ± 0.24 for contribution-guided selection (Only B5) and 50.82 ± 0.40 for the full-parameter baseline (+0.53 over Full, capturing 8% of the total RL training gain). On Qwen3-4B-Base, the heuristic achieves 64.80 ± 0.30 vs. 65.87 ± 0.70 (Only B5) and 62.97 ± 0.78 (Full), a +1.83 improvement representing 17% of the total RL gain. On Qwen3-8B-Base, 68.19 ± 0.62 vs. 68.97 ± 0.31 (Only B5) and 66.43 ± 0.40 (Full), a +1.76 improvement representing 21% of the total RL gain. Across all three scales, the

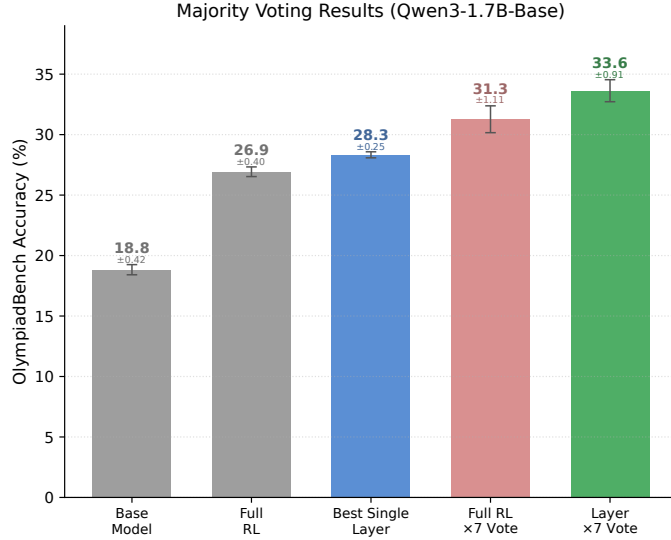


Figure 8: Majority voting results on OlympiadBench (Qwen3-1.7B-Base). Voting across 7 diverse layer-trained models surpasses both the best single-layer model and the full-parameter baseline, and also exceeds self-consistency-style voting over 7 samples from the same full-parameter model. Error bars denote one standard deviation over 3 independent evaluation runs.

heuristic surpasses the full-parameter baseline without any per-layer profiling, and achieves a substantial portion of the improvement of contribution-guided selection.

This result has a practical implication: when even a single round of per-layer profiling is unavailable, simply training the middle layers provides a strong default strategy that captures a meaningful portion of the benefit of contribution-guided selection.

5 Discussion

5.1 Diversity in Layer-Trained Models

In §3 we showed that layer contribution varies dramatically across layers. Among the high-contribution layers, however, some layer-trained models’ performance is comparable. For example, on Qwen3-1.7B-Base, the top-7 layers all achieve OlympiadBench accuracy between 23% and 28%. A natural question is whether these similarly-performing models solve the same problems or different ones. We investigate this below to better understand what has been learned in layer training.

High-contribution layers solve different subsets of problems. We train each of the 28 layers of Qwen3-1.7B-Base independently (as in §3.2) and evaluate all resulting models on OlympiadBench. For each of the top-7 high-contribution layers, we record the set of problems its model newly solves relative to the base model, and measure pairwise overlap via the Jaccard similarity $J(A, B) = |A \cap B| / |A \cup B|$, where A and B are problems solved by two different layer-trained models. The average pairwise Jaccard similarity is only 34.1%: despite comparable accuracy, these models solve largely non-overlapping sets of problems. For instance, the Layer 10 and Layer 13 models reach 27.3% and 28.3% accuracy respectively, but share only 31.9% of their newly-solved problems. This indicates that each high-contribution layer captures a different aspect of RL-induced improvement, and the knowledge they encode is complementary rather than redundant.

Majority voting quantifies this complementarity. To measure the practical value of this complementarity, we aggregate the predictions of the top-7 layer-trained models via majority voting on OlympiadBench. The ensemble reaches $33.6 \pm 0.91\%$, surpassing both the best individual layer-trained model ($28.3 \pm 0.25\%$) and the full-parameter baseline ($26.9 \pm 0.40\%$) by a substantial margin (Figure 8). To isolate the role of *structural* diversity from sampling randomness, we compare against self-consistency-style voting [Wang et al., 2023], which aggregates 7 independent samples from the same full-parameter model; this reaches only $31.3 \pm 1.11\%$, confirming that diversity arising from

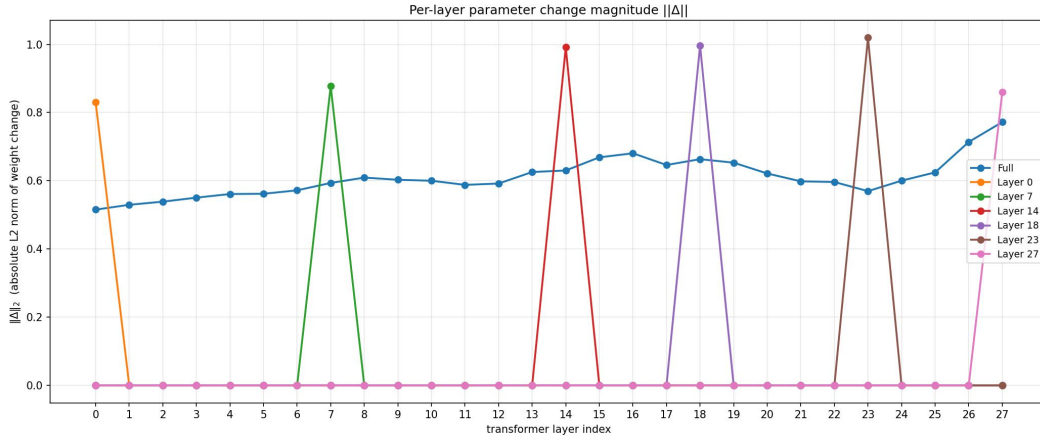


Figure 9: Per-layer weight change magnitude $\|\Delta\theta_k\|_2$ on Qwen3-1.7B-Base. Blue: full-parameter training (all layers change). Colored spikes: single-layer training (only the trained layer changes; all others remain at zero). Under full training, the weight change is relatively uniform across layers, contrasting with the highly non-uniform layer contribution profile. Under single-layer training, all trained layers undergo comparable weight changes regardless of their contribution, indicating that layer contribution reflects the effectiveness of a layer’s parameter subspace rather than the magnitude of parameter change.

training distinct layers is more effective than diversity from repeated sampling. This connects to the observation by Gan and Isola [2026] that diverse task-specific experts are densely distributed around pretrained weights: single-layer training provides a structured way to reach such experts along an interpretable axis—transformer depth.

Finally, we emphasize that the layer-wise training and majority voting framework is intended as an analysis tool rather than a practical training strategy, since it requires independently training multiple layer-specific models. Nevertheless, this analysis provides valuable insights into the diversity of representations learned by different transformer layers and their respective contributions to RL post-training. These insights, in turn, motivate the more practical layer-aware training strategies developed in Section 4.

5.2 Weight Change Magnitude vs. Layer Contribution

A natural question is whether high-contribution layers are simply layers whose parameters change more during the full-parameter training. For example, in the extreme case if after full training, only the middle layer moves while the rest of the layers stay unchanged, then of course our observation of middle-layer contribution is trivial. To investigate this, we measure the per-layer weight change magnitude $\|\Delta\theta_k\|_2$ (L2 norm of the difference between trained and base-model parameters) for both full-parameter training and several representative single-layer training runs on Qwen3-1.7B-Base (Figure 9).

Two observations stand out. First, under full-parameter training, the weight change magnitude is remarkably uniform across layers (ranging from approximately 0.5 to 0.8), despite the highly non-uniform layer contribution profile observed in §3.2. This dissociation indicates that layer contribution is not explained by how much a layer’s parameters change during training, as middle layers do not change more than other layers in full training, yet they contribute far more when trained in isolation.

Second, under single-layer training, the trained layer undergoes a substantially larger weight change than the same layer experiences during full training (approximately 0.8–1.0 vs. 0.5–0.7). This suggests that when a single layer must absorb all RL-induced improvement, it compensates by moving further in parameter space. Crucially, however, the magnitude of this single-layer weight change is similar across layers with very different contribution values: both high-contribution and low-contribution layers undergo comparable weight changes when trained alone, yet produce vastly different performance outcomes. This reinforces the conclusion that layer contribution reflects the *effectiveness* of a layer’s parameter subspace for capturing RL improvement, rather than the *magnitude* of parameter change.

6 Related Work

Layer Importance in LLMs. Several works have studied the roles of individual layers in LLMs. Song et al. [2026] analyze layer importance through pruning, finding that removing certain layers causes performance to collapse while removing others has little effect. Zhang et al. [2024] identify “cornerstone layers” whose removal reduces performance to near random guessing, and Nepal et al. [2025] show that the critical layers for mathematical reasoning are determined during pretraining and remain invariant after post-training. In the context of parameter-efficient finetuning, LISA [Pan et al., 2024] proposes randomly sampling layers to update during SFT, and MISA [Liu et al., 2026] extends this with importance-aware sampling. AdaGradSelect [Kumar et al., 2025] uses gradient statistics to dynamically select which layers to train during SFT. These works primarily operate in inference-time analysis or the supervised finetuning setting. In contrast, our work focuses on the RL setting and demonstrates that layer contribution is a stable property that generalizes across datasets and tasks, enabling principled layer selection without per-dataset profiling.

Diverse Solutions in Weight Space. Gan and Isola [2026] discover that the neighborhood around pretrained weights contains dense, diverse task-specific experts that can be found through random perturbation. Our findings provide a new perspective: single-layer training offers a structured way to explore this neighborhood, with each layer accessing a different region of the solution space. The diversity among layer-trained models is evidenced by their low pairwise agreement and effective majority voting.

7 Conclusion

In this work, we investigate how different layers in LLMs respond to RL post-training. Through systematic single-layer training experiments across seven models spanning two model families (Qwen3, Qwen2.5), three RL algorithms (GRPO, GiGPO, Dr. GRPO), and two task domains (mathematical reasoning and agentic decision-making), we discover that layers differ dramatically in their capacity to capture RL-induced improvement. High-contribution layers consistently concentrate in the middle of the network, and this variation is a stable structural property determined by the model itself rather than by the specific dataset, task, or algorithm used for training.

We show that this property has direct practical value: prioritizing high-contribution layers through adaptive learning rates or selective training consistently outperforms standard uniform RL, and even a simple heuristic that trains only the middle layers surpasses full-parameter training without any per-layer profiling. Beyond guiding training, we find that high-contribution layers capture complementary aspects of RL-induced improvement, and that the magnitude of weight change does not explain the variation in layer contribution—layers that change equally in parameter space produce vastly different performance outcomes.

Our work has several limitations. Our guided training strategies are validated only on mathematical reasoning; extending them to coding and agentic tasks is left for future work. Additionally, our layer contribution metric is defined with respect to a specific training configuration, and a deeper theoretical understanding of why middle layers are disproportionately important for RL adaptation remains an open question.

References

- Lang Feng, Zhenghai Xue, Tingcong Liu, and Bo An. Group-in-group policy optimization for llm agent training, 2025. URL <https://arxiv.org/abs/2505.10978>.
- Yulu Gan and Phillip Isola. Neural thickets: Diverse task experts are dense around pretrained weights, 2026. URL <https://arxiv.org/abs/2603.12228>.
- Daya Guo, Dejian Yang, Haowei Zhang, Junxiao Song, Peiyi Wang, Qihao Zhu, Runxin Xu, Ruoyu Zhang, Shirong Ma, Xiao Bi, Xiaokang Zhang, Xingkai Yu, Yu Wu, Z. F. Wu, Zhibin Gou, Zhihong Shao, Zhuoshu Li, Ziyi Gao, Aixin Liu, Bing Xue, Bingxuan Wang, Bochao Wu, Bei Feng, Chengda Lu, Chenggang Zhao, Chengqi Deng, Chong Ruan, Damai Dai, Deli Chen, Dongjie Ji, Erhang Li, Fangyun Lin, Fucong Dai, Fuli Luo, Guangbo Hao, Guanting Chen, Guowei Li, H. Zhang, Hanwei Xu, Honghui Ding, Huazuo Gao, Hui Qu, Hui Li, Jianzhong Guo, Jiashi Li, Jingchang Chen, Jingyang Yuan, Jinhao Tu, Junjie Qiu, Junlong Li, J. L. Cai, Jiaqi Ni, Jian Liang, Jin Chen, Kai Dong, Kai Hu, Kaichao You, Kaige Gao, Kang Guan, Kexin Huang, Kuai Yu, Lean Wang, Lecong Zhang, Liang Zhao, Litong Wang, Liyue Zhang, Lei Xu, Leyi Xia, Mingchuan Zhang, Minghua Zhang, Minghui Tang, Mingxu Zhou, Meng Li, Miaojun Wang, Mingming Li, Ning Tian, Panpan Huang, Peng Zhang, Qiancheng Wang, Qinyu Chen, Qiushi Du, Ruiqi Ge, Ruisong Zhang, Ruizhe Pan, Runji Wang, R. J. Chen, R. L. Jin, Ruyi Chen, Shanghao Lu, Shangyan Zhou, Shanhuang Chen, Shengfeng Ye, Shiyu Wang, Shuiping Yu, Shunfeng Zhou, Shuting Pan, S. S. Li, Shuang Zhou, Shaoqing Wu, Tao Yun, Tian Pei, Tianyu Sun, T. Wang, Wangding Zeng, Wen Liu, Wenfeng

- Liang, Wenjun Gao, Wenqin Yu, Wentao Zhang, W. L. Xiao, Wei An, Xiaodong Liu, Xiaohan Wang, Xiaokang Chen, Xiaotao Nie, Xin Cheng, Xin Liu, Xin Xie, Xingchao Liu, Xinyu Yang, Xinyuan Li, Xuecheng Su, Xuheng Lin, X. Q. Li, Xiangyue Jin, Xiaojin Shen, Xiaosha Chen, Xiaowen Sun, Xiaoxiang Wang, Xinnan Song, Xinyi Zhou, Xianzu Wang, Xinxia Shan, Y. K. Li, Y. Q. Wang, Y. X. Wei, Yang Zhang, Yanhong Xu, Yao Li, Yao Zhao, Yaofeng Sun, Yaohui Wang, Yi Yu, Yichao Zhang, Yifan Shi, Yiliang Xiong, Ying He, Yishi Piao, Yisong Wang, Yixuan Tan, Yiyang Ma, Yiyuan Liu, Yongqiang Guo, Yuan Ou, Yuduan Wang, Yue Gong, Yuheng Zou, Yujia He, Yunfan Xiong, Yuxiang Luo, Yuxiang You, Yuxuan Liu, Yuyang Zhou, Y. X. Zhu, Yanping Huang, Yaohui Li, Yi Zheng, Yuchen Zhu, Yunxian Ma, Ying Tang, Yukun Zha, Yuting Yan, Z. Z. Ren, Zehui Ren, Zhangli Sha, Zhe Fu, Zhean Xu, Zhenda Xie, Zhengyan Zhang, Zhewen Hao, Zhicheng Ma, Zhigang Yan, Zhiyu Wu, Zihui Gu, Zijia Zhu, Zijun Liu, Zilin Li, Ziwei Xie, Ziyang Song, Zizheng Pan, Zhen Huang, Zhipeng Xu, Zhongyu Zhang, and Zhen Zhang. Deepseek-r1 incentivizes reasoning in llms through reinforcement learning. *Nature*, 645(8081):633–638, 2025. ISSN 1476-4687. doi: 10.1038/s41586-025-09422-z. URL <http://dx.doi.org/10.1038/s41586-025-09422-z>.
- Jujie He, Jiakai Liu, Chris Yuhao Liu, Rui Yan, Chaojie Wang, Peng Cheng, Xiaoyu Zhang, Fuxiang Zhang, Jiacheng Xu, Wei Shen, Siyuan Li, Liang Zeng, Tianwen Wei, Cheng Cheng, Bo An, Yang Liu, and Yahui Zhou. Skywork open reasoner 1 technical report, 2025. URL <https://arxiv.org/abs/2505.22312>.
- Anshul Kumar, Gagan Raj Gupta, and Manisha Chawla. Adagradselect: An adaptive gradient-guided layer selection method for efficient fine-tuning of slms, 2025. URL <https://arxiv.org/abs/2512.15764>.
- Jia LI, Edward Beeching, Lewis Tunstall, Ben Lipkin, Roman Soletskyi, Shengyi Costa Huang, Kashif Rasul, Longhui Yu, Albert Jiang, Ziju Shen, Zihan Qin, Bin Dong, Li Zhou, Yann Fleureau, Guillaume Lample, and Stanislas Polu. NuminaMath. [<https://huggingface.co/AI-MO/NuminaMath-CoT>] (https://github.com/project-numina/aimo-progress-prize/blob/main/report/numina_dataset.pdf), 2024.
- Yuxi Liu, Renjia Deng, Yutong He, Xue Wang, Tao Yao, and Kun Yuan. Misa: Memory-efficient llms optimization with module-wise importance sampling, 2026. URL <https://arxiv.org/abs/2511.00056>.
- Zichen Liu, Changyu Chen, Wenjun Li, Penghui Qi, Tianyu Pang, Chao Du, Wee Sun Lee, and Min Lin. Understanding r1-zero-like training: A critical perspective. In *Second Conference on Language Modeling*, 2025. URL <https://openreview.net/forum?id=5PAF7PAY2Y>.
- Michael Luo, Sijun Tan, Roy Huang, Ameen Patel, Alpay Ariyak, Qingyang Wu, Xiaoxiang Shi, Rachel Xin, Colin Cai, Maurice Weber, Ce Zhang, Li Erran Li, Raluca Ada Popa, and Ion Stoica. DeepCoder: A fully open-source 14b coder at o3-mini level. <https://pretty-radio-b75.notion.site/DeepCoder-A-Fully-Open-Source-14B-Coder-at-O3-mini-Level-1cf81902c14680b3bee5eb349a512a51>, 2025a. Notion Blog.
- Michael Luo, Sijun Tan, Justin Wong, Xiaoxiang Shi, William Tang, Manan Roongta, Colin Cai, Jeffrey Luo, Tianjun Zhang, Erran Li, Raluca Ada Popa, and Ion Stoica. DeepScaler: Surpassing o1-preview with a 1.5b model by scaling rl. <https://pretty-radio-b75.notion.site/DeepScaleR-Surpassing-O1-Preview-with-a-1-5B-Model-by-Scaling-RL-19681902c1468005bed8ca303013a4e2>, 2025b. Notion Blog.
- Aadim Nepal, Safal Shrestha, Anubhav Shrestha, Minwu Kim, Jalal Naghiyev, Ravid Shwartz-Ziv, and Keith Ross. Layer importance for mathematical reasoning is forged in pre-training and invariant after post-training, 2025. URL <https://arxiv.org/abs/2506.22638>.
- Rui Pan, Xiang Liu, Shizhe Diao, Renjie Pi, Jipeng Zhang, Chi Han, and Tong Zhang. Lisa: Layerwise importance sampling for memory-efficient large language model fine-tuning, 2024. URL <https://arxiv.org/abs/2403.17919>.
- Zhihong Shao, Peiyi Wang, Qihao Zhu, Runxin Xu, Junxiao Song, Xiao Bi, Haowei Zhang, Mingchuan Zhang, Y. K. Li, Y. Wu, and Daya Guo. Deepseekmath: Pushing the limits of mathematical reasoning in open language models, 2024. URL <https://arxiv.org/abs/2402.03300>.
- Guangyuan Shi, Zexin Lu, Xiaoyu Dong, Wenlong Zhang, Xuanyu Zhang, Yujie Feng, and Xiao-Ming Wu. Understanding layer significance in llm alignment, 2025. URL <https://arxiv.org/abs/2410.17875>.
- Mohit Shridhar, Xingdi Yuan, Marc-Alexandre Côté, Yonatan Bisk, Adam Trischler, and Matthew Hausknecht. Alford: Aligning text and embodied environments for interactive learning, 2021. URL <https://arxiv.org/abs/2010.03768>.
- Xinyuan Song, Keyu Wang, PengXiang Li, Lu Yin, and Shiwei Liu. Demystifying the roles of llm layers in retrieval, knowledge, and reasoning, 2026. URL <https://arxiv.org/abs/2510.02091>.
- Xuezhi Wang, Jason Wei, Dale Schuurmans, Quoc Le, Ed Chi, Sharan Narang, Aakanksha Chowdhery, and Denny Zhou. Self-consistency improves chain of thought reasoning in language models, 2023. URL <https://arxiv.org/abs/2203.11171>.

An Yang, Anfeng Li, Baosong Yang, Beichen Zhang, Binyuan Hui, Bo Zheng, Bowen Yu, Chang Gao, Chengen Huang, Chenxu Lv, Chujie Zheng, Dayiheng Liu, Fan Zhou, Fei Huang, Feng Hu, Hao Ge, Haoran Wei, Huan Lin, Jialong Tang, Jian Yang, Jianhong Tu, Jianwei Zhang, Jianxin Yang, Jiayi Yang, Jing Zhou, Jingren Zhou, Junyang Lin, Kai Dang, Keqin Bao, Kexin Yang, Le Yu, Lianghai Deng, Mei Li, Mingfeng Xue, Mingze Li, Pei Zhang, Peng Wang, Qin Zhu, Rui Men, Ruize Gao, Shixuan Liu, Shuang Luo, Tianhao Li, Tianyi Tang, Wenbiao Yin, Xingzhang Ren, Xinyu Wang, Xinyu Zhang, Xuancheng Ren, Yang Fan, Yang Su, Yichang Zhang, Yinger Zhang, Yu Wan, Yuqiong Liu, Zekun Wang, Zeyu Cui, Zhenru Zhang, Zhipeng Zhou, and Zihan Qiu. Qwen3 technical report, 2025. URL <https://arxiv.org/abs/2505.09388>.

Qiyang Yu, Zheng Zhang, Ruofei Zhu, Yufeng Yuan, Xiaochen Zuo, Yu Yue, Weinan Dai, Tiantian Fan, Gaohong Liu, Lingjun Liu, Xin Liu, Haibin Lin, Zhiqi Lin, Bole Ma, Guangming Sheng, Yuxuan Tong, Chi Zhang, Mofan Zhang, Wang Zhang, Hang Zhu, Jinhua Zhu, Jiase Chen, Jiangjie Chen, Chengyi Wang, Hongli Yu, Yuxuan Song, Xiangpeng Wei, Hao Zhou, Jingjing Liu, Wei-Ying Ma, Ya-Qin Zhang, Lin Yan, Mu Qiao, Yonghui Wu, and Mingxuan Wang. Dapo: An open-source llm reinforcement learning system at scale, 2025. URL <https://arxiv.org/abs/2503.14476>.

Yang Zhang, Yanfei Dong, and Kenji Kawaguchi. Investigating layer importance in large language models, 2024. URL <https://arxiv.org/abs/2409.14381>.

Appendix

A Training Details and Hyperparameters

A.1 Overview

Table 1 in the main text summarizes all seven models and their training configurations. Below we provide full hyperparameter details for each experimental setup. In all cases, single-layer training freezes every parameter except the target decoder layer (including the embedding layer and the language model head), and follows the same hyperparameters as the corresponding full-parameter baseline unless otherwise noted.

A.2 Qwen3 Models (GRPO, NuminaMath-CoT)

All Qwen3 experiments are conducted using the veRL framework with GRPO as the RL algorithm and AdamW as the optimizer. We use Qwen3-1.7B-Base (28 layers), Qwen3-4B-Base (36 layers), and Qwen3-8B-Base (36 layers) as base models.

For single-layer training, each layer is trained independently on NuminaMath-CoT (downsampled to 50K problems after decontamination). The full-parameter baseline uses identical hyperparameters but with all layers unfrozen. Table 8 summarizes the key hyperparameters. For the full-parameter baselines, we tune the learning rate over $\{1 \times 10^{-6}, 3 \times 10^{-6}, 5 \times 10^{-6}, 1 \times 10^{-5}\}$ and report the best result (with learning rate = 5×10^{-6}); For single-layer training, we use a learning rate of 5×10^{-6} , which aligns with the full-parameter training. For the adaptive learning rate experiments in §4.1, the boosted learning rate is set to 1×10^{-5} and the base rate to 5×10^{-6} .

Table 8: Training hyperparameters for Qwen3 models (GRPO, NuminaMath-CoT).

Hyperparameter	Value
RL Algorithm	GRPO
Learning Rate	5×10^{-6}
Train Batch Size	512
PPO Mini Batch Size	128
PPO Micro Batch Size	8
Group Size (G)	4
Max Response Length	3072
KL Coefficient	0.001
Clip Range (ϵ)	0.2
Epochs	4

A.3 Qwen2.5-Math-1.5B (Dr. GRPO)

The generalization experiment in §3.4 follows the Dr. GRPO recipe of Liu et al. [2025], implemented in the Oat framework. We RL-tune Qwen2.5-Math-1.5B with the unbiased Dr. GRPO objective, which removes the response-length ($1/|o_i|$) and question-level (std) normalization terms from the GRPO objective. Training uses the MATH training set with a binary answer-matching reward verified by Math-Verify. The single-layer training protocol is identical to §3.2: we train one decoder layer at a time while freezing all other parameters, and for each layer we report the best checkpoint by average score. Table 9 lists the hyperparameters. Similar to the Qwen3 experiments, for the full-parameter baselines, we tune the learning rate over $\{1 \times 10^{-6}, 3 \times 10^{-6}, 5 \times 10^{-6}, 1 \times 10^{-5}\}$ and report the best result (with learning rate = 5×10^{-6}); For single-layer training, we use a learning rate of 5×10^{-6} , which aligns with the full-parameter training.

For evaluation we use six mathematics benchmarks—AIME 2024, AIME 2025, AMC, MATH500, Minerva Math, and OlympiadBench—and report layer contribution $\mathcal{C}(k)$ on their unweighted average (Avg6). This evaluation suite follows the setup associated with the Dr. GRPO recipe and differs from the benchmark suite used for the Qwen3 experiments.

Table 9: Training hyperparameters for Qwen2.5-Math-1.5B (Dr. GRPO).

Hyperparameter	Value
RL Algorithm	Dr. GRPO
Learning Rate	5×10^{-6}
Train Batch Size	128
Group Size (G)	8
Max Response Length	3072
KL Coefficient	0
Clip Range (ϵ)	0.2
Epochs	8

A.4 Qwen2.5-Instruct Models (GiGPO, ALFWorld)

The agentic experiments in §3.4 use Qwen2.5-1.5B-Instruct (28 layers) and Qwen2.5-3B-Instruct (36 layers) trained with GiGPO on ALFWorld, an environment-based agentic benchmark consisting of 2,435 household tasks across six categories (Pick&Place, Pick&Place with two objects, Examine in Light, Heat&Place, Cool&Place, Clean&Place). The reward is binary: 1 if the agent successfully completes the task, 0 otherwise. Table 10 lists the hyperparameters. Similar to the Qwen3 experiments, for the full-parameter baselines, we tune the learning rate over $\{1 \times 10^{-6}, 3 \times 10^{-6}, 5 \times 10^{-6}, 1 \times 10^{-5}\}$ and report the best result (with learning rate = 5×10^{-6}); For single-layer training, we use a learning rate of 5×10^{-6} , which aligns with the full-parameter training.

Table 10: Training hyperparameters for Qwen2.5-Instruct models (GiGPO, ALFWorld).

Hyperparameter	Value
RL Algorithm	GiGPO
Learning Rate	5×10^{-6}
Train Batch Size	256
PPO Mini Batch Size	256
PPO Micro Batch Size	32
Group Size (G)	8
Max Response Length	512
KL Coefficient	0.01
Clip Range (ϵ)	0.2
Steps	150

A.5 DeepSeek-Distilled-Qwen-7B (GRPO, Skywork-OR1)

To test generalization beyond the Qwen model families, we train DeepSeek-R1-Distill-Qwen-7B (28 layers), a model distilled from DeepSeek-R1 into the Qwen architecture, using GRPO on the Skywork-OR1 mathematics dataset

(approximately 48K problems). The reward is binary answer-matching. Table 11 lists the hyperparameters. Similar to the Qwen3 experiments, for the full-parameter baselines, we tune the learning rate over $\{1 \times 10^{-6}, 3 \times 10^{-6}, 5 \times 10^{-6}, 1 \times 10^{-5}\}$ and report the best result (with learning rate = 5×10^{-6}); For single-layer training, we use a learning rate of 5×10^{-6} , which aligns with the full-parameter training.

Table 11: Training hyperparameters for DeepSeek-Distilled-Qwen-7B (GRPO, Skywork-OR1).

Hyperparameter	Value
RL Algorithm	GRPO
Learning Rate	5×10^{-6}
Train Batch Size	256
PPO Mini Batch Size	128
PPO Micro Batch Size	2
Group Size (G)	8
Max Response Length	16384
KL Coefficient	0
Clip Range (ϵ)	0.2
Epochs	8

A.6 Training Datasets

NuminaMath-CoT. Our primary training dataset is derived from NuminaMath-CoT [LI et al., 2024], a large-scale collection of approximately 860K competition-level math problems with chain-of-thought solutions, sourced from Chinese high school exams, US and international mathematics olympiads, and online mathematics forums. To improve training efficiency, we randomly downsample the dataset to 50K problems. We apply strict decontamination filtering to prevent test set leakage: for each of our evaluation benchmarks, we remove any training problem whose question text has a high n-gram overlap or semantic similarity with any test problem. The reward is binary: 1 if the model’s final answer matches the ground truth, 0 otherwise.

DeepScaleR. A curated mathematics dataset containing approximately 40K reasoning-intensive problems [Luo et al., 2025b], compiled from sources including AIME, AMC, and other competition archives. Used for cross-dataset validation in §3.3. The same binary answer-matching reward is applied.

DeepCoder. A coding dataset containing approximately 24K programming problems with test cases [Luo et al., 2025a], compiled from LiveCodeBench and Codeforces. Used for cross-task validation in §3.3. The reward is based on execution correctness: 1 if the generated code passes all test cases, 0 otherwise.

Skywork-OR1. A mathematics dataset containing approximately 48K problems. Used for training DeepSeek-Distilled-Qwen-7B in §3.4. The same binary answer-matching reward is applied.

ALFWorld. An environment-based agentic benchmark consisting of 2,435 household tasks across six categories. Each task requires the agent to interact with a simulated environment through text commands to achieve a goal (e.g., placing a heated object on a surface). The reward is binary: 1 if the task is completed successfully, 0 otherwise. Used for training the Qwen2.5-Instruct models in §3.4.

A.7 Learning Rate Ablation

A natural concern is whether the layer contribution rankings observed in §3.2 are artifacts of the learning rate choice—specifically, whether low-contribution layers might perform better with a larger learning rate, or whether high-contribution layers might lose their advantage under a different learning rate. We address this with the following ablation.

On Qwen3-1.7B-Base, we select the top-5 and bottom-5 layers by contribution ranking and retrain each of them individually with a $3\times$ higher learning rate (1.5×10^{-5} vs. the default 5×10^{-6}), keeping all other hyperparameters unchanged. Table 12 shows the results. The bottom-5 layers remain low-contribution under the boosted learning rate: their \mathcal{C} values change by at most 0.02, and none of them approaches the high-contribution group. Similarly, the top-5 layers retain their high contribution under the same boosted learning rate. This confirms that the layer

contribution profile is robust to the learning rate choice and is not an artifact of suboptimal hyperparameters, supporting the conclusion in §3.3 that layer contribution is an intrinsic property of the model.

Table 12: Learning rate ablation on Qwen3-1.7B-Base. We compare layer contribution \mathcal{C} of the top-5 and bottom-5 layers (by contribution ranking) under the default learning rate (5×10^{-6}) and a $3\times$ boosted learning rate (1.5×10^{-5}). Low-contribution layers remain low-contribution and high-contribution layers remain high-contribution under the higher learning rate.

Group	Layer	\mathcal{C} (LR= 5×10^{-6})	\mathcal{C} (LR= 1.5×10^{-5})
Top-5	Layer 10	1.14	1.12
	Layer 12	1.12	1.13
	Layer 9	1.04	1.01
	Layer 2	1.03	1.00
	Layer 13	1.01	1.02
Bottom-5	Layer 24	0.28	0.26
	Layer 20	0.32	0.34
	Layer 23	0.32	0.33
	Layer 25	0.35	0.35
	Layer 26	0.36	0.35

B Benchmark Selection Criteria

We evaluate on 12 benchmarks grouped into four categories. Here we describe each benchmark and our selection criteria.

Math (in-domain).

- **MATH500**: 500 competition-level math problems spanning algebra, geometry, number theory, and more.
- **GSM8K**: 8.5K grade-school math word problems requiring multi-step arithmetic reasoning.
- **OlympiadBench**: Olympiad-level mathematics problems.
- **AMC**: Problems from the American Mathematics Competitions. **Considering the dataset is very small, we report the Average@32 results of evaluation on AMC.**

Code (out-of-distribution).

- **HumanEval+**: Function-level code generation with augmented test cases.
- **MBPP**: Mostly Basic Python Programs, testing basic programming ability.
- **LiveCodeBench**: Recent competitive programming problems collected after model training cutoff dates.

Reasoning (out-of-distribution).

- **GPQA-Diamond**: Graduate-level science questions curated by domain experts.
- **MMLU-Pro**: An enhanced version of MMLU with harder, more discriminative questions.

Language (out-of-distribution).

- **C-Eval**: A comprehensive Chinese evaluation benchmark covering diverse subjects.
- **IFEval**: Instruction-following evaluation measuring the model’s ability to follow specific formatting and content constraints.
- **MGS**: Multilingual Grade School Math evaluates multilingual mathematical reasoning.

C Full Per-Layer Results

Tables 13, 14, and 15 provide the complete per-layer evaluation results of Qwen3 models for all 12 benchmarks on each model scale. Table 16 provide the complete per-layer evaluation results for all 6 benchmarks on Qwen2.5-Math-1.5B.

Table 13: Full per-layer results for Qwen3-1.7B-Base. \mathcal{C} denotes layer contribution on math.

Setting	MATH500	GSM8K	Olymp.	AMC	Math	HE+	MBPP	LCB	Code	GPQA	MMLU-P	Reas.	C-Eval	IFEval	MGSM	Lang.	Overall	\mathcal{C}
Base	57.4	74.4	18.7	26.1	44.1	44.5	52.9	7.4	34.9	5.6	35.7	20.7	47.5	30.1	47.5	41.7	35.4	0.00
Full	64.0	82.0	26.9	30.2	50.8	43.3	46.3	10.9	33.5	5.0	40.1	22.6	56.2	32.4	56.0	48.2	38.8	1.00
Layer 0	63.4	81.7	23.6	31.9	50.1	46.3	55.6	10.9	37.6	5.0	39.5	22.3	54.9	31.6	51.8	46.1	39.0	0.89
Layer 1	64.4	79.4	25.9	30.2	50.0	55.5	55.2	9.1	40.0	6.6	38.8	22.7	55.4	34.9	51.0	47.1	39.9	0.87
Layer 2	67.8	80.0	26.1	30.5	51.1	42.7	53.7	10.9	35.7	6.1	39.5	22.8	55.7	32.4	52.0	46.7	39.1	1.03
Layer 3	62.2	79.8	24.6	30.0	49.1	47.0	49.4	12.6	36.3	4.0	39.1	21.6	54.4	35.7	50.9	47.0	38.5	0.75
Layer 4	61.2	81.3	25.5	29.2	49.3	44.5	51.8	10.3	35.5	5.0	38.7	21.9	54.0	33.1	51.8	46.3	38.3	0.77
Layer 5	63.4	79.8	24.4	29.8	49.3	41.5	53.7	8.0	34.4	4.5	39.0	21.8	52.5	31.2	51.6	45.1	37.7	0.78
Layer 6	63.8	80.4	25.6	30.0	50.0	48.8	51.0	9.1	36.3	3.5	39.0	21.3	54.4	31.6	53.5	46.5	38.5	0.87
Layer 7	64.0	80.1	24.9	29.0	49.5	47.0	53.7	13.7	38.1	6.1	38.8	22.4	54.5	31.4	53.6	46.5	39.1	0.80
Layer 8	62.4	79.8	25.0	28.7	49.0	45.7	51.8	10.3	35.9	3.5	39.0	21.3	51.3	29.9	53.5	44.9	37.8	0.72
Layer 9	65.8	81.7	24.6	32.4	51.1	45.7	51.4	10.9	36.0	4.0	39.8	21.9	54.7	31.4	54.6	46.9	39.0	1.04
Layer 10	68.6	80.5	27.3	30.8	51.8	40.9	53.7	9.1	34.6	5.0	38.7	21.9	55.6	31.1	54.9	47.2	38.9	1.14
Layer 11	64.0	81.8	26.1	29.4	50.3	43.3	55.6	12.0	37.0	2.5	39.0	20.8	54.2	31.2	54.1	46.5	38.6	0.92
Layer 12	65.6	81.3	27.3	32.4	51.6	42.7	52.9	13.1	36.2	7.1	39.4	23.2	55.7	32.2	55.2	47.7	39.7	1.12
Layer 13	64.6	79.7	28.3	31.0	50.9	34.1	53.7	11.4	33.1	4.0	40.5	22.3	57.4	30.1	55.0	47.5	38.4	1.01
Layer 14	64.4	79.6	27.1	30.0	50.3	40.9	53.7	10.3	34.9	4.0	40.4	22.2	55.4	29.6	53.6	46.2	38.4	0.92
Layer 15	63.2	81.5	26.1	31.4	50.5	34.8	55.2	14.3	34.8	6.6	38.8	22.7	56.9	31.8	55.3	48.0	39.0	0.95
Layer 16	64.8	80.9	23.0	30.8	49.9	37.2	52.5	8.6	32.8	3.0	39.4	21.2	56.0	32.4	54.1	47.5	37.8	0.85
Layer 17	63.6	79.5	26.2	29.6	49.7	31.7	51.0	12.6	31.8	8.6	39.3	23.9	55.3	29.4	51.8	45.5	37.7	0.83
Layer 18	61.8	78.5	24.3	29.7	48.6	34.1	49.4	12.6	32.0	6.1	39.3	22.7	52.4	29.8	51.9	44.7	37.0	0.66
Layer 19	59.8	77.9	23.1	29.6	47.6	34.8	51.4	8.6	31.6	4.5	38.0	21.3	51.8	28.1	52.4	44.1	36.1	0.52
Layer 20	60.6	74.9	21.6	28.1	46.3	31.7	51.0	9.7	30.8	6.1	37.2	21.6	52.4	29.6	50.0	44.0	35.7	0.32
Layer 21	60.6	75.0	24.3	27.4	46.8	38.4	47.9	11.4	32.6	7.1	38.4	22.8	52.1	28.1	51.2	43.8	36.5	0.40
Layer 22	60.6	76.5	24.3	27.9	47.3	35.4	51.8	8.6	31.9	4.5	36.7	20.6	51.9	28.8	51.9	44.2	36.0	0.47
Layer 23	60.6	73.5	22.4	28.6	46.3	30.5	54.5	10.3	31.8	5.6	37.2	21.4	52.5	30.5	50.2	44.4	36.0	0.32
Layer 24	60.6	74.8	21.2	27.6	46.1	29.9	50.6	11.4	30.6	6.1	37.1	21.6	52.8	29.8	50.0	44.2	35.6	0.28
Layer 25	60.8	74.2	22.7	28.3	46.5	24.4	51.4	9.7	28.5	6.6	37.7	22.1	50.2	30.9	50.6	43.9	35.3	0.35
Layer 26	60.6	74.4	23.4	27.8	46.5	29.3	51.0	9.1	29.8	4.0	36.8	20.4	52.4	27.0	50.2	43.2	35.0	0.36
Layer 27	61.8	75.8	25.0	28.3	47.7	25.0	51.0	9.1	28.4	4.5	37.5	21.0	51.6	28.6	50.6	43.6	35.2	0.54

Table 14: Full per-layer results for Qwen3-4B-Base. \mathcal{C} denotes layer contribution on math.

Setting	MATH500	GSM8K	Olymp.	AMC	Math	HE+	MBPP	LCB	Code	GPQA	MMLU-P	Reas.	C-Eval	IFEval	MGSM	Lang.	Overall	\mathcal{C}
Base	65.2	75.4	27.6	40.5	52.2	68.3	44.8	11.4	41.5	5.1	52.5	28.8	69.9	39.7	63.2	57.6	45.0	0.00
Full	77.2	91.9	38.4	47.1	63.7	69.5	63.0	13.7	48.8	6.6	58.1	32.4	71.7	40.5	76.5	62.9	51.9	1.00
Layer 0	77.8	88.3	35.3	42.8	61.0	72.6	68.9	13.7	51.7	4.5	56.8	30.7	68.9	48.8	71.6	63.1	51.6	0.77
Layer 1	74.0	87.7	36.4	42.7	60.2	70.7	67.3	12.6	50.2	6.1	55.2	30.6	71.1	46.2	72.9	63.4	51.1	0.70
Layer 2	73.8	87.7	35.3	42.4	59.8	69.5	63.0	14.9	49.1	8.6	55.3	31.9	69.9	45.7	71.3	62.3	50.8	0.66
Layer 3	74.4	87.5	36.3	42.5	60.2	70.1	57.2	15.4	47.6	9.1	55.1	32.1	68.6	44.4	72.1	61.7	50.4	0.70
Layer 4	74.2	88.0	37.9	43.1	60.8	67.1	61.1	15.4	47.9	4.5	54.7	29.6	68.4	43.4	72.7	61.5	49.9	0.75
Layer 5	76.6	86.3	37.0	44.3	61.1	65.2	61.1	13.1	46.5	8.6	55.5	32.0	69.3	46.4	71.5	62.4	50.5	0.77
Layer 6	77.0	89.5	38.8	44.4	62.4	68.9	63.8	14.9	49.2	5.0	55.9	30.5	71.5	43.1	74.4	63.0	51.3	0.89
Layer 7	73.8	89.4	39.1	44.1	61.6	68.9	64.2	14.9	49.3	7.6	55.8	31.7	72.0	41.6	73.3	62.3	51.2	0.82
Layer 8	75.2	90.5	36.6	45.0	61.8	68.3	65.0	16.0	49.8	5.6	55.4	30.5	70.7	42.0	74.2	62.3	51.1	0.84
Layer 9	77.2	89.3	37.0	44.9	62.1	68.9	61.5	13.7	48.0	4.0	55.9	30.0	70.8	42.9	73.8	62.5	50.7	0.87
Layer 10	76.2	90.8	39.6	44.9	62.8	68.9	61.9	12.0	47.6	6.6	56.1	31.4	70.3	43.4	75.3	63.0	51.2	0.93
Layer 11	76.6	90.5	36.2	47.6	62.7	73.2	66.5	14.3	51.3	11.1	56.4	33.8	71.0	41.6	75.8	62.8	52.7	0.92
Layer 12	80.8	90.4	37.0	45.6	63.4	69.5	66.5	13.7	49.9	7.6	56.8	32.2	70.2	42.9	75.3	62.8	52.1	0.98
Layer 13	76.8	89.5	38.1	44.8	62.3	69.5	66.5	13.1	49.7	6.6	56.8	31.7	70.4	41.6	76.1	62.7	51.6	0.88
Layer 14	78.4	90.3	39.9	46.5	63.8	73.8	70.0	14.9	52.9	5.0	58.1	31.6	71.8	42.1	76.0	63.3	52.9	1.02
Layer 15	78.0	90.8	39.0	46.2	63.5	70.1	64.6	13.7	49.5	6.1	57.7	31.9	72.1	46.0	76.6	64.9	52.4	0.98
Layer 16	79.4	92.0	40.3	45.5	64.3	75.0	66.5	14.3	51.9	8.1	57.9	33.0	73.8	42.3	77.1	64.4	53.4	1.06
Layer 17	78.4	91.0	38.8	45.9	63.5	74.4	65.0	17.1	52.2	6.1	57.9	32.0	71.5	43.4	77.1	64.0	52.9	0.99
Layer 18	78.6	90.5	37.9	45.5	63.1	67.1	69.7	15.4	50.7	7.1	57.5	32.3	72.6	43.6	77.0	64.4	52.6	0.96
Layer 19	78.0	91.4	40.3	45.6	63.8	70.1	66.2	14.3	50.2	6.1	57.7	31.9	73.1	42.0	76.6	63.9	52.5	1.02
Layer 20	79.0	90.7	39.0	43.6	63.1	68.9	66.2	16.6	50.5	6.6	58.1	32.3	71.3	41.6	75.8	62.9	52.2	0.95
Layer 21	76.2	89.9	39.6	45.5	62.8	65.2	67.3	17.7	50.1	7.6	57.5	32.6	74.2	41.6	75.6	63.8	52.3	0.93
Layer 22	78.0	90.8	39.3	46.5	63.6	68.3	64.2	16.0	49.5	6.1	58.0	32.0	70.7	41.2	75.9	62.6	51.9	1.00
Layer 23	76.8	90.5	37.5	44.9	62.4	67.1	65.4	16.0	49.5	7.6	56.8	32.2	70.7	40.7	75.5	62.3	51.6	0.89
Layer 24	77.0	89.5	38.5	43.6	62.2	72.0	58.4	12.0	47.4	7.6	56.3	31.9	70.7	39.6	74.8	61.7	50.8	0.87
Layer 25	76.6	89.0	36.0	44.4	61.5	70.7	57.2	16.0	48.0	7.6	56.4	32.0	71.5	40.9	73.9	62.1	50.9	0.81
Layer 26	73.8	89.7	35.9	44.3	60.9	69.5	56.0	16.6	47.4	5.0	56.4	30.7	71.9	40.3	75.0	62.4	50.3	0.76
Layer 27	75.6	89.5	34.2	43.5	60.7	70.7	55.6	13.1	46.5	7.1	56.7	31.9	70.2	39.7	73.7	61.2	50.1	0.74
Layer 28	75.6	89.0	35.7															

Table 15: Full per-layer results for Qwen3-8B-Base. \mathcal{C} denotes layer contribution on math.

Setting	MATH500	GSM8K	Olymp.	AMC	Math	HE+	MBPP	LCB	Code	GPQA	MMLU-P	Reas.	C-Eval	IFEval	MGSM	Lang.	Overall	\mathcal{C}
Base	71.8	82.0	36.6	41.7	58.0	67.1	66.9	17.1	50.4	6.6	57.7	32.2	71.5	46.2	54.8	57.5	49.5	0.00
Full	80.0	92.3	42.8	50.8	66.5	75.6	67.3	18.3	53.7	8.1	63.0	35.5	70.1	47.7	73.3	63.7	54.9	1.00
Layer 0	61.8	79.6	31.0	42.4	53.7	66.5	49.0	16.6	44.0	7.6	60.3	34.0	73.1	46.4	69.5	63.0	48.7	-0.51
Layer 1	72.2	84.7	36.3	45.8	59.7	72.6	65.8	16.0	51.4	8.6	60.1	34.3	72.3	49.4	67.3	63.0	52.1	0.20
Layer 2	72.8	84.6	38.5	43.0	59.7	73.2	67.3	13.7	51.4	7.1	60.3	33.7	71.9	45.5	60.8	59.4	51.1	0.20
Layer 3	77.8	89.3	37.0	48.6	63.2	78.0	68.9	18.3	55.1	9.1	60.0	34.6	72.7	47.3	68.1	62.7	53.9	0.61
Layer 4	73.6	84.8	39.0	49.6	61.7	76.8	70.8	18.3	55.3	9.6	60.4	35.0	76.2	48.4	62.9	62.5	53.6	0.44
Layer 5	76.8	88.7	40.4	49.0	63.7	78.0	68.5	14.9	53.8	10.1	60.8	35.5	75.4	48.6	65.3	63.1	54.0	0.67
Layer 6	79.0	90.1	40.0	50.7	65.0	76.8	73.9	17.7	56.2	8.1	62.3	35.2	74.4	54.5	68.5	65.8	55.5	0.82
Layer 7	79.4	88.5	40.1	48.6	64.2	73.8	73.5	16.6	54.6	9.6	61.7	35.6	73.7	49.5	66.7	63.3	54.4	0.72
Layer 8	77.0	89.0	41.5	50.9	64.6	72.0	71.6	19.4	54.3	7.1	61.8	34.4	73.8	46.6	65.6	62.0	53.8	0.78
Layer 9	80.4	90.9	41.2	51.5	66.0	71.3	72.4	17.1	53.6	5.6	61.2	33.4	71.9	46.6	65.4	61.3	53.6	0.94
Layer 10	78.6	90.6	41.0	51.5	65.4	79.3	69.3	16.6	55.0	9.1	61.8	35.4	73.7	49.4	72.2	65.1	55.3	0.87
Layer 11	75.4	84.5	37.2	49.9	61.7	79.9	71.2	17.1	56.1	9.1	61.7	35.4	71.0	47.7	52.6	57.1	52.6	0.44
Layer 12	77.8	90.8	39.4	52.2	65.1	76.8	69.7	18.3	54.9	5.6	61.6	33.6	75.8	48.1	70.2	64.7	54.6	0.83
Layer 13	80.8	90.5	41.0	51.7	66.0	78.0	68.5	15.4	54.0	8.1	62.0	35.0	74.6	48.1	65.4	62.7	54.4	0.94
Layer 14	81.6	92.6	41.2	51.8	66.8	80.5	70.0	16.6	55.7	5.0	62.4	33.7	75.2	51.0	76.3	67.5	55.9	1.03
Layer 15	79.8	92.8	40.6	52.7	66.5	78.7	73.5	18.3	56.8	5.0	63.0	34.0	77.0	51.9	77.8	68.9	56.5	1.00
Layer 16	80.4	91.8	44.1	52.0	67.1	76.2	72.4	14.9	54.5	7.6	63.5	35.5	76.1	52.5	77.8	68.8	56.5	1.07
Layer 17	81.6	92.5	41.6	52.5	67.1	76.2	70.4	16.0	54.2	6.6	63.1	34.9	74.9	49.5	76.6	67.0	55.8	1.07
Layer 18	80.6	92.0	39.6	51.2	65.8	76.8	71.2	13.7	53.9	9.6	63.1	36.3	75.0	45.7	74.0	64.9	55.2	0.92
Layer 19	79.6	91.8	43.0	50.7	66.3	72.6	68.9	18.3	53.2	9.6	62.6	36.1	72.8	48.2	72.8	64.6	55.1	0.97
Layer 20	77.2	92.3	41.2	51.3	65.5	68.9	64.6	17.7	50.4	9.1	62.2	35.7	73.3	44.9	70.8	63.0	53.6	0.88
Layer 21	79.8	92.4	41.5	49.9	65.9	71.3	68.1	15.4	51.6	8.6	62.0	35.3	74.3	47.5	69.0	63.6	54.1	0.93
Layer 22	80.8	91.2	41.9	51.2	66.3	70.7	64.6	17.1	50.8	6.1	62.3	34.2	74.0	45.3	72.7	64.0	53.8	0.98
Layer 23	80.8	90.2	42.5	50.4	66.0	70.1	62.6	17.1	50.0	9.1	61.4	35.2	69.0	42.1	68.6	59.9	52.8	0.94
Layer 24	79.8	91.1	41.2	49.7	65.5	70.1	60.7	16.6	49.1	7.1	60.9	34.0	70.3	43.6	66.7	60.2	52.2	0.88
Layer 25	78.0	89.4	39.4	48.0	63.7	70.7	58.8	18.9	49.4	7.6	60.8	34.2	72.4	44.0	69.0	61.8	52.3	0.67
Layer 26	77.0	89.2	38.2	49.0	63.3	68.9	58.8	18.9	48.8	7.1	60.6	33.8	69.2	43.4	65.0	59.2	51.3	0.63
Layer 27	80.8	88.8	41.0	49.2	65.0	74.4	59.1	16.0	49.8	8.6	61.0	34.8	69.9	44.5	66.8	60.4	52.5	0.82
Layer 28	79.0	88.6	41.2	48.3	64.3	72.6	58.8	17.1	49.5	7.1	60.9	34.0	70.6	43.4	67.8	60.6	52.1	0.74
Layer 29	78.8	87.9	39.4	47.5	63.4	68.9	58.0	15.4	47.4	9.1	61.0	35.0	72.1	45.1	65.2	60.8	51.7	0.64
Layer 30	78.6	88.2	38.1	48.8	63.4	68.9	56.4	13.7	46.3	9.6	60.9	35.3	69.8	46.0	63.3	59.7	51.2	0.64
Layer 31	77.4	88.9	40.0	50.3	64.2	75.0	53.3	18.3	48.9	9.6	60.3	34.9	69.7	45.3	60.5	58.5	51.6	0.72
Layer 32	71.8	85.4	38.1	46.1	60.3	54.9	47.1	15.4	39.1	9.1	58.0	33.5	66.5	46.0	61.5	58.0	47.8	0.27
Layer 33	78.0	87.6	39.3	48.2	63.3	70.1	35.0	16.0	40.4	7.1	60.6	33.8	68.0	46.6	66.6	60.4	49.5	0.62
Layer 34	77.6	87.0	39.7	48.8	63.3	60.4	40.5	17.1	39.3	7.1	59.6	33.3	63.1	38.3	73.5	58.3	48.6	0.62
Layer 35	78.4	88.9	41.2	49.3	64.5	60.4	29.2	18.3	35.9	7.6	61.0	34.3	67.8	33.6	70.5	57.3	48.0	0.76

Table 16: Full per-layer results for Qwen2.5-Math-1.5B (Dr. GRPO). \mathcal{C} denotes layer contribution on Avg.

Setting	AIME	AIME25	AMC	MATH500	Minerva	Olymp.	Avg	\mathcal{C}
Base	20.0	6.7	32.5	33.0	12.5	22.8	21.2	0.00
Full	16.7	10.0	51.8	74.4	25.0	38.8	36.1	1.00
Layer 0	10.0	10.0	47.0	70.4	23.2	33.9	32.4	0.75
Layer 1	10.0	6.7	49.4	68.2	20.2	31.6	31.0	0.66
Layer 2	10.0	3.3	44.6	71.2	21.7	32.6	30.6	0.63
Layer 3	20.0	10.0	45.8	69.8	21.3	33.0	33.3	0.81
Layer 4	13.3	3.3	44.6	70.4	23.2	32.7	31.2	0.67
Layer 5	16.7	3.3	44.6	69.4	22.4	32.1	31.4	0.68
Layer 6	6.7	6.7	43.4	69.2	22.1	31.6	29.9	0.59
Layer 7	6.7	6.7	42.2	69.0	20.6	30.2	29.2	0.54
Layer 8	13.3	3.3	43.4	69.4	20.6	30.7	30.1	0.60
Layer 9	20.0	3.3	43.4	69.8	23.2	33.0	32.1	0.73
Layer 10	13.3	6.7	44.6	70.4	23.2	32.6	31.8	0.71
Layer 11	16.7	3.3	44.6	69.6	21.7	32.3	31.4	0.68
Layer 12	20.0	10.0	45.8	73.8	25.0	34.8	34.9	0.92
Layer 13	13.3	10.0	45.8	69.6	22.8	34.4	32.6	0.77
Layer 14	20.0	10.0	52.3	74.8	25.6	35.3	36.3	1.01
Layer 15	16.7	10.0	43.4	73.8	26.1	36.7	34.4	0.89
Layer 16	20.0	10.0	51.8	75.2	24.9	34.9	36.1	1.00
Layer 17	16.7	6.7	49.4	73.4	24.6	35.3	34.3	0.88
Layer 18	10.0	0.0	49.4	71.0	24.6	34.1	31.5	0.69
Layer 19	10.0	0.0	45.8	70.4	22.8	31.7	30.1	0.60
Layer 20	10.0	0.0	45.8	64.6	20.2	30.7	28.5	0.49
Layer 21	13.3	3.3	45.8	67.2	19.1	29.6	29.7	0.57
Layer 22	13.3	0.0	37.3	65.2	19.9	30.5	27.7	0.43
Layer 23	10.0	3.3	38.6	64.0	19.9	29.3	27.5	0.42
Layer 24	16.7	3.3	37.3	65.2	21.0	29.9	28.9	0.51
Layer 25	16.7	3.3	41.0	62.4	19.1	28.1	28.4	0.48
Layer 26	13.3	3.3	42.2	66.2	20.6	29.9	29.2	0.54
Layer 27	10.0	6.7	42.2	69.4	24.3	32.3	30.8	0.64